Parity doublets and the pairing mechanism in C_{60}

R. Friedberg and T. D. Lee
Columbia University, New York, New York 10027

H. C. Ren
The Rockefeller University, New York, New York 10021

(Received 27 March 1992; revised manuscript received 23 June 1992)

We show that the near degeneracy of the low-lying vector (T_{1u}) and axial-vector (T_{1g}) levels in an isolated C_{60}^- can provide a simple pairing mechanism in C_{60}^{2-}, C_{60}^{3-}, and the K_nC_{60} crystal. This gives rise to the possibility of a "boson" band in K_nC_{60}, in addition to the usual fermion bands. The implications for superconductivity are discussed.

I. INTRODUCTION

The discovery of C_{60} and the superconductivity of its alloy compounds[1-4] provide a rich field for new theoretical and experimental investigations.[5-8] In this paper we show that the near degeneracy of the low-lying vector (T_{1u}) and axial-vector (T_{1g}) levels of an isolated C_{60}^- ion may provide a simple pairing mechanism in C_{60}^{2-}, C_{60}^{3-}, and the K_nC_{60} crystal.

We begin with a review of the single-electron energy levels of a C_{60} molecule in the next section. Above the 60 closed shell lie two triplets possessing the same icosahedral symmetry label T_1 but of opposite parity. We derive their wave functions in the tight-binding limit of the molecular-orbit approximation and exhibit these functions in a simple and useful form, which prompts us to refer to them as "vector" and "axial vector." Our analysis is then extended to C_{60}^{2-}. By taking into account the strong Coulomb energy between electrons, we find that the spectrum of C_{60}^{2-} contains two low-lying states invariant under the proper icosahedral symmetry transformations, but again of opposite parity and hence naturally called "scalar" and "pseudoscalar," with an energy degeneracy within 1% of their excitation energy (in our approximate calculation), even closer than the vector axial-vector doublets in C_{60}^-. The details of this remarkable feature are analyzed in Sec. III.

Since parity doublets, two states of opposite parity with nearly the same energy, are not a common occurrence in physics, we sketch below the mechanism that gives rise to them in C_{60}. (For a microscopic system, such as mesons and baryons, composite particles of opposite parities usually have quite different internal structures, which make them unlikely to be degenerate. In most macroscopic systems, as in the case of left- or right-handed sugar molecules, it is conceptually simple to construct coherent mixtures of opposite parities that are nearly degenerate; the difficulty lies in the practical realization of such coherent mixtures.)

Set the C_{60} molecule on a unit sphere. The radial position vector $\hat{\mathbf{g}}$ of each C atom on the sphere corresponds to an element g of the proper icosahedral group. Thus the 60-dimensional Hilbert space of the tight-binding limit supports the regular representation of this group. For a typical "hopping" Hamiltonian of icosahedral symmetry, the lowest single-particle state is that having a constant wave function, reminiscent of the s wave (i.e., the orbital angular momentum quantum number $l=0$) on a sphere. In the icosahedral group, this singlet representation is labeled A or, more fully, A_g (the subscript $g=$*gerade*, meaning even parity).

The next-lowest state has a threefold degeneracy (excluding spin), which may be described as follows. For each C atom, it turns out that there is a certain unit vector $\hat{\mathbf{e}}_0(g)$, very close to $\hat{\mathbf{g}}$, within an angle of about 1°; as will be shown in Sec. III, the wave function at site $\hat{\mathbf{g}}$ can be chosen to be proportional to $\hat{\mathbf{e}}_0(g)\cdot\hat{\mathbf{n}}$, where $\hat{\mathbf{n}}$ is some fixed vector. Clearly, one obtains in this way three independent wave functions of the same energy, corresponding to the three independent choices of $\hat{\mathbf{n}}$. If we approximate $\hat{\mathbf{e}}_0(g)\cong\hat{\mathbf{g}}$ (as we shall do hereafter in this section), then these three states correspond to the p-wave triplet ($l=1$) on the sphere. Under the icosahedral group, this triplet representation is labeled T_1 or, more fully, T_{1u} ($u=$*ungerade*, meaning odd parity, since $\hat{\mathbf{g}}$ changes sign for oppositely placed C atoms).

It is natural to call the singlet and triplet states described above "scalar" and "vector," referring to the way they transform when the laboratory coordinate system is rotated or inverted. Thus the designation "vector" refers to the vector $\hat{\mathbf{n}}$, which selects a T_1 state. Since multiplicity and parity play a prominent role in our analysis, we shall write 1^+ (scalar) for A_g, 3^- (vector) for T_{1u}, etc., with 1^+ denoting a singlet of even parity, 3^- a triplet of odd parity, etc. (All these multiplicities are doubled by spin.)

In the regular representation, each irreducible representation of dimension d appears d times; thus, the triplet T_1 must appear 3 times. Our interest will be in the *other* two triplets T_1, whose energy lies far above that of the "p-wave" state described above. Their wave functions can be expressed simply as follows.

Because of the detailed structure of the molecule, each C atom defines not only a radial vector $\hat{\mathbf{g}}$, but a local

coordinate system, with its three orthonormal basis vectors denoted by

$$\hat{\mathbf{g}},\ \hat{\mathbf{e}}_-(g),\ \text{and}\ \hat{\mathbf{e}}_+(g)\ , \tag{1.1}$$

where

$$\hat{\mathbf{e}}_+(g)=\hat{\mathbf{g}}\times\hat{\mathbf{e}}_-(g)\ . \tag{1.2}$$

Under an inversion, $\hat{\mathbf{g}}$ changes sign; consequently, $\hat{\mathbf{e}}_-(g)$ and $\hat{\mathbf{e}}_+(g)$ are of opposite parities. Let $\hat{\mathbf{e}}_-(g)$ be of odd parity; then, $\hat{\mathbf{e}}_+(g)$ is of even parity. By taking the wave function proportional to $\hat{\mathbf{e}}_-(g)\cdot\hat{\mathbf{n}}$ (where, as before, $\hat{\mathbf{n}}$ is some fixed vector), one obtains a triplet 3^- or T_{1u}, the lowest-unoccupied molecular-orbit (LUMO) state in neutral C_{60}. By taking $\hat{\mathbf{e}}_+(g)\cdot\hat{\mathbf{n}}$, one obtains a 3^+ or T_{1g}, the second LUMO state in neutral C_{60}. It is natural to call these triplets "vector" and "axial vector," respectively. Together, (1.1) determines the set of three triplets T_1 contained in the regular representation.

To transform a C atom to one of its nearest neighbors by an element of the icosahedral group, one must rotate through a large angle (180° for one of the nearest neighbors), about an axis rather close to $\hat{\mathbf{g}}$. Hence $\hat{\mathbf{g}}$ varies slowly between neighbors, but, as we shall see, $\hat{\mathbf{e}}_-(g)$ and $\hat{\mathbf{e}}_+(g)$ vary rapidly and, because of (1.2), by about the same amount. This is why the $\hat{\mathbf{e}}_-\cdot\hat{\mathbf{n}}$ and $\hat{\mathbf{e}}_+\cdot\hat{\mathbf{n}}$ triplets have energy far above that of the $\hat{\mathbf{g}}\cdot\hat{\mathbf{n}}$ triplet, but close to each other. (Although the high-lying 3^- and 3^+ states have the same formal structure under the *icosahedral group* as the low-lying 3^-, if one attempts to fill in a smooth wave function between the C atoms, one will need mostly spherical harmonics of $l=5$ and 6 for $\hat{\mathbf{e}}_-$ and $\hat{\mathbf{e}}_+$, respectively, instead of $l=1$ as for $\hat{\mathbf{g}}$.)

Since $\hat{\mathbf{e}}_-\cdot\hat{\mathbf{n}}$ and $\hat{\mathbf{e}}_+\cdot\hat{\mathbf{n}}$ are the two low-lying levels above the 60 closed shell, in C_{60}^- the extra electron may be in either of these triplets. The nearness of these two levels of opposite parity, combined with their compatibility (both T_1) under the icosahedral group, render C_{60}^- highly polarizable, as will be calculated in Sec. III.

In C_{60}^{2-}, the Coulomb energy between the two extra electrons plays a dominant role. Without this term the lowest-energy state would be of the form $T_{1u}T_{1u}$ or $3^-\times3^-$. But we find that two other states have considerably lower Coulomb energy. One is obtained by combining T_{1u} and T_{1g} to make a two-particle state 1^-:

$$T_{1u}T_{1g}+T_{1g}T_{1u}\ \text{ with wave function}$$
$$[\hat{\mathbf{e}}_-(g)\cdot\hat{\mathbf{e}}_+(g')+\hat{\mathbf{e}}_+(g)\cdot\hat{\mathbf{e}}_-(g')](\uparrow\downarrow'-\downarrow\uparrow')\ . \tag{1.3}$$

The other is made by mixing the 1^+ combination of $T_{1u}T_{1u}$ with that of $T_{1g}T_{1g}$:

$$T_{1u}T_{1u}+T_{1g}T_{1g}\ \text{ with wave function}$$
$$[\hat{\mathbf{e}}_-(g)\cdot\hat{\mathbf{e}}_-(g')-\hat{\mathbf{e}}_+(g)\cdot\hat{\mathbf{e}}_+(g')](\uparrow\downarrow'-\downarrow\uparrow')\ , \tag{1.4}$$

where $\hat{\mathbf{g}}$, $\uparrow$, or $\downarrow$ and $\hat{\mathbf{g}}'$, $\uparrow'$, or $\downarrow'$ are the position and spin variables of the two electrons. Because both wave functions vanish when the two electrons coalesce ($\hat{\mathbf{g}}=\hat{\mathbf{g}}'$), their mutual Coulomb energy is greatly reduced; this leads to the spin-0 parity doublets in C_{60}^{2-}, labeled 1^- and 1^+.

The wave functions (1.3) and (1.4) represent singlets in both position and spin; no external vector $\hat{\mathbf{n}}$ appears. It is natural to call these paired states "pseudoscalar" and "scalar." It is evident that if the energy difference $\Delta\varepsilon$ between $3^-(T_{1u})$ and $3^+(T_{1g})$ is small, then it will contribute only to order $(\Delta\varepsilon)^2$ to the splitting between scalar and pseudoscalar paired states. This is why the paired states in C_{60}^{2-} form a much tighter parity doublet than the component one-particle states in C_{60}^-.

The closeness of these parity doublets makes it natural to isolate their response to strong interactions, separate from other distant levels. This provides a convenient means to derive analytical expressions for many of the important parts of strong-interaction effects. Thus we can calculate the polarization energy of C_{60}^- in a strong electric field E, showing that it changes from the weak-field expression $-\frac{1}{2}\alpha E^2$ to one that depends linearly on E. Another example is to derive the final energy in C_{60}^{2-}, within the parity-doublet approximation, to all powers of the interaction Hamiltonian. (As one of the applications, these closed expressions can be used to test the validity of some calculations made in the literature,[8] which are based on a second-order perturbation in the interaction energy, as will be discussed below and also in Sec. IV.)

In Sec. V we turn our attention to the K_3C_{60} crystal and first calculate the Madelung energy. The result shows that all K atoms are ionized, as is commonly accepted.

Above the 60 closed shell, a typical band calculation reveals a low-lying cluster of three overlapping narrow bands, which is the Bloch wave extension of the three components of the vector wave function $\hat{\mathbf{e}}_-(g)$ of an isolated C_{60}^- ion. These overlapping fermion bands are half filled in the case of K_3C_{60}. On the other hand, the pseudoscalar pairing wave function (1.3) in C_{60}^{2-} suggests a different Bloch wave extension, one that represents the hopping of such a highly correlated two-particle state in the crystal. The orthogonality of these correlated two-particle Bloch wave functions to any product of two one-particle wave functions in the fermion bands follows from the original orthogonality condition in a single C_{60} molecule:

$$\sum_{g=1}^{60}\hat{\mathbf{e}}_-(g)_i\hat{\mathbf{e}}_+(g)_j=0\ , \tag{1.5}$$

where i and j denote the vector components. We call the Bloch extension of (1.3) the "boson band" (or the pseudoscalar band).

The two electrons in the fermion bands have an energy advantage over the boson on account of the excitation energy $\Delta\varepsilon$ and the lowering in kinetic energy; however, there is a disadvantage to the fermion bands of having a higher Coulomb energy. The important question concerning the role of bosons versus fermions depends on the delicate balance between these two opposing factors. This is examined in Sec. VI. We start with the Coulomb

energy (~ 11 eV per lattice cell) between three electrons in the fermion bands and compare that with the configuration of placing two electrons in the boson band and the remaining one in the fermion bands. We then take into account the kinetic-energy and van der Waals energy differences; the latter is important because of the large polarizability of the C_{60} negative ion. The final energy balance between these two configurations is estimated to be only 0.22 eV, slightly in favor of the fermion bands. However, considering the highly approximate nature of our calculations and that the final answer is only about 2% of the initial energy that we begin with, it is not possible to make any definitive statement. Nevertheless, a variety of interesting theoretical possibilities emerges. It seems likely that there exists a narrow boson band, which may lie very close to or overlapping with, the three fermion bands.

The possibility of a close-by low-lying boson band, in addition to the usual fermion bands, has important consequences for superconductivity. The bosons may undergo Bose-Einstein condensation. The zero-momentum nature of the Bose condensate necessarily generates charge fluctuations in the coordinate space; thereby, it increases the Coulomb energy. In Sec. VII we show that this Coulomb-energy increase is compensated for, at near distances, by the monopole-dipole interaction between neighboring C_{60} molecules because of their large polarizability. At large distances there is, in addition, the Debye screening of the Coulomb potential generated by these charge fluctuations.

In Sec. VIII, through a simplified but explicit field-theoretic model, we are able to examine the effect of the Bloch extension of the correlated scalar wave function (1.4), the parity-doublet partner of the pseudoscalar (1.3). Except in the somewhat unlikely case that the boson band is lower in energy than 2 times the bottom energy of the fermion bands, the scalar only provides a resonance to the electrons in the fermion bands. Such a resonance can produce an energy gap, as in the BCS theory of superconductivity. While both members of the bosonic parity doublet can be important to superconductivity, their roles are different, as will be discussed in Sec. IX. The experimentally observed pressure variation of the critical temperature[6] is shown to be consistent with the model.

All the calculations made in this paper neglect the effect of levels outside the parity doublet, as an approximation. Alternatively, Chakravarty, Gelfand, and Kivelson[8] calculate an energy balance favorable to pairing by including all levels, but only perturbatively. As we shall show in Sec. IV C, this calculation is not quantitatively reliable because the failure of perturbation theory for the parity doublet alone causes an error comparable to the calculated pairing energy. Nevertheless the pairing mechanism of Ref. 8 does exist in principle.

Our thesis is that the $3^{+}(T_{1g})$ level plays a special role because of its coupling and near degeneracy with the $3^{-}(T_{1u})$ at the Fermi level. Therefore the C_{60}^{2-} energy should be calculated by starting with the mixed states of (1.3) and (1.4) and treating all levels *outside* the parity doublet perturbatively. This last step, which we do not carry out here, would probably add a significant term to the pairing energy.

In either case we think that the parity doublets provide an essential insight into the nature of the paired wave function in C_{60}, as well as the physics associated with polarizability of the C_{60} negative ion.

In this paper superconductivity is discussed on the basis of a simplified model Hamiltonian given by (8.8) in Sec. VIII, in which there is an effective "attractive and local" four-fermion field interaction term (8.7). Its presence is due to the lowering of the strong Coulomb energy in the correlated paired states (1.3) and (1.4) in C_{60}^{2-}, which, in turn, can be justified within the parity-doublet approximation. On the other hand, parity doublets are rather special to C_{60}; a natural question is to ask how important are their roles to superconductivity in general. We believe that, for superconductors with very small coherence length, the essential common feature probably lies in the approximate applicability of an effective "attractive and local" interaction term, such as the ones in (8.7). For material other than C_{60}, its underlying reason may have nothing to do with parity doublets. The parity doublets of C_{60} simply provide a convenient tool for us to penetrate the maze of strong interactions.

II. MOLECULAR ORBITS OF C_{60}

A. Icosahedral group

In order to have the necessary tools for our subsequent analysis, we give a brief discussion of the molecular orbits of C_{60}. As will be shown below, these can be expressed in terms of the regular representation of the proper

$$\text{icosahedral group } \mathcal{G}=\{g\}\ , \tag{2.1}$$

where g denotes its 60 group elements. Corresponding to the identity element e, we may take any point $\hat{\mathbf{e}}$ on a unit sphere with center 0. The application of the finite rotation that associates with g transforms $\hat{\mathbf{e}}$ to $\hat{\mathbf{g}}$. For $\hat{\mathbf{e}}$ not lying on any of the symmetry axes, the resulting 60 $\hat{\mathbf{g}}$ are all different. (A convenient notation is to use the same $\hat{\mathbf{e}}$ and $\hat{\mathbf{g}}$ to denote the corresponding unit radial vectors of the sphere, as well as their end points on the sphere.) For definiteness, let the unit sphere be the *circumsphere* of a regular icosahedron of vertices $N, A_1, \ldots, A_5', S$. As in Fig. 1, choose the point e (corresponding to the identity element e in $\mathcal{G}$) on the edge $\overline{A_1N}$, with $\overline{eN}=\frac{1}{3}\overline{A_1N}$ and $\mathbf{0e}\|\hat{\mathbf{e}}$. Each unit radial vector $\hat{\mathbf{g}}$ intersects a point g on one of the edges of the icosahedron. The location of each point g, thus generated, gives the position of a carbon nucleus in the C_{60} molecule, provided the unit scale of the radius is $R\cong 4.03$ Å, so that the circumspherical radius of the C_{60} molecule is its actual value $R_0\cong 3.5$ Å, with the ratio

$$\frac{R}{R_0}=3\left[5+\frac{4}{\sqrt{5}}\right]^{-1/2}\simeq 1.15\ . \tag{2.2}$$

(The same notation g denotes both the group element as well as the position of the carbon nucleus.) Any function $f(g)$ of these 60 positions g can be expressed in terms of

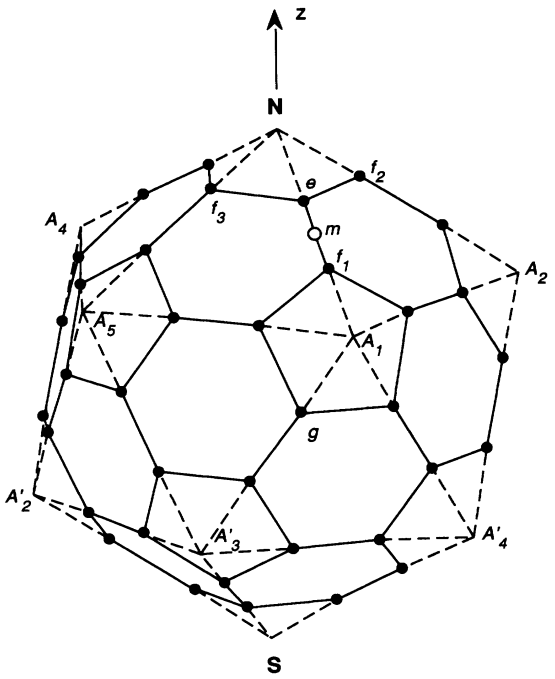

FIG. 1. Set on a unit sphere the 12 vertices of an icosahedron: N, S, A_i, and A_i' ($i=1,2,\ldots,5$), with $\overline{NS}$ and $\overline{A_iA_i'}$ the diameters of the sphere whose center is 0. Each of the 60 dots $e, f_1, f_2, f_3, g, \ldots$ denote the positions of C atoms in C_{60}. The three nearest neighbors of e are f_1, f_2, and f_3. The distance $\overline{ef_2}=\overline{ef_3}$ is slightly different from $\overline{ef_1}$. In the molecular-orbit calculation, e.g., (2.25) and (3.1), these three nearest neighbors are treated on an equal basis, as an approximation.

the irreducible representations of the icosahedral group $\mathcal{G}$, which consist of a singlet **1**, two triplets **3** and $\tilde{\mathbf{3}}$, a quartet **4**, and a quintet **5**. This gives

$$60=1^2+3^2+3^2+4^2+5^2 . \tag{2.3}$$

In the literature[9,10] these representations are often referred to as A, T_1, T_2, G, and H, respectively. Our notations follow those used in particle physics, with the dimensionality of the irreducible representation shown explicitly.

The irreducible representations **1**, **3**, and **5** can be readily identified with the usual $l=0$ (s wave), $l=1$ (p wave), and $l=2$ (d wave) of the spherical harmonics $Y_{l,m}(\theta,\phi)$, where $m=-l,-l+1,\ldots,l$ and θ and ϕ are the polar and azimuthal angles, respectively. To derive the remaining two irreducible representations $\tilde{\mathbf{3}}$ and **4** we designate one of the icosahedral vertices as the north pole N ($\theta=0$), as in Fig. 1. Express any function F of θ,ϕ defined on the 12 vertices of the icosahedron in terms of the 16 spherical harmonics: $l=0$, 1, 2, and 3 of $Y_{l,m}(\theta,\phi)$. (Note that $16=1+3+5+7$.) On the other hand, the function F has only

$$12=1+3+5+3 \tag{2.4}$$

values. Hence we expect four linear combinations of the seven $l=3$ $Y_{l,m}(\theta,\phi)$ to be identically zero on these 12 icosahedral vertices, leaving a triplet $\tilde{\mathbf{3}}$. For an explicit construction, we observe that the geodesic arc between two nearest-neighboring vertices of an icosahedron is $\cos^{-1}(1/\sqrt{5})$; therefore,

$$Y_{3,\pm1}(\theta,\phi)\propto(5\cos^2\theta-1)\sin\theta e^{\pm i\phi} \tag{2.5}$$

is zero on all these 12 vertices. Likewise, on these sites,

$$Y_{3,\pm3}(\theta,\phi)\propto Y_{3,\mp2}(\theta,\phi) , \tag{2.6}$$

from which we can readily form two linear combinations of these $l=3$ spherical harmonics that are also zero. In (2.6) both sides have the azimuthal variation because of the fivefold symmetry along the north-pole–south-pole diameter; hence, (2.6) holds in the northern hemisphere, since, excluding the pole, all the other five icosahedral vertices are at the same latitude. Its validity in the southern hemisphere then follows from inversion symmetry. In this way we see that under the icosahedral rotations the seven $Y_{3,m}(\theta,\phi)$ functions decompose into a quartet **4** and another triplet $\tilde{\mathbf{3}}$, different from **3**.

Returning to the C_{60} structure on the unit sphere, we denote by $|g\rangle$ a vector (*ket* vector in Dirac's notation) with 60 components. Each element g corresponds to a definite finite rotation of the icosahedral group, which can be specified by its three Eulerian angles $\omega=(\alpha,\beta,\gamma)$. Let $|\mathbf{d},M,\Lambda\rangle$ be the *ket* vector whose components are those of the regular representation (in terms of the irreducible representations **d** with **d**=**1**, **3**, $\tilde{\mathbf{3}}$, **4**, and **5**). The transformation matrix relating $|g\rangle$ to $|\mathbf{d},M,\Lambda\rangle$ is

$$\langle g|\mathbf{d},M,\Lambda\rangle\equiv\left[\frac{d}{N}\right]^{1/2}T^{\mathbf{d}}_{M\Lambda}(\alpha,\beta,\gamma) , \tag{2.7}$$

where $\langle g|$ is the *bra* vector dual to $|g\rangle$, $N=60$ is the dimensionality of the regular representation, and d is the dimension of the representation **d**. For **d**=**1**, **3**, and **5**, the matrices $T^{\mathbf{d}}_{M\Lambda}(\alpha,\beta,\gamma)$ are simply the standard transformation matrices in a rigid body, i.e.,

$$T^{\mathbf{d}}_{M\Lambda}(\alpha,\beta,\gamma)=D^{J}_{M\Lambda}(\alpha,\beta,\gamma) , \tag{2.8}$$

with $J=0$, 1, and 2 (i.e., $d=2J+1$). The matrices $D^J_{M\Lambda}(\alpha,\beta,\gamma)$ relate the spherical harmonics $Y_{J,M}$ in the laboratory frame to the corresponding $Y_{J,\Lambda}$ in the body frame. In (2.7), M and Λ can vary independently over d values and, for **d**=**1**, **3**, and **5**, from $-J$ to J. Thus, in accordance with (2.3), each irreducible representation (characterized by **d** and M) appears d times in the regular representation, depending on the value of Λ. Regarding (2.7) as a 60×60 matrix, we have the unitarity conditions

$$\sum_g\langle\mathbf{d},M,\Lambda|g\rangle\langle g|\mathbf{d}',M',\Lambda'\rangle=\delta_{\mathbf{d}\mathbf{d}'}\delta_{MM'}\delta_{\Lambda\Lambda'} \tag{2.9}$$

and

$$\sum_{\mathbf{d},M,\Lambda}\langle g|\mathbf{d},M,\Lambda\rangle\langle\mathbf{d},M,\Lambda|g'\rangle=\delta gg' , \tag{2.10}$$

where δ_{ab} is the Kronecker symbol.

The inversion operator $\mathcal{J}$ commutes with $\mathcal{G}$ and changes

$$\hat{\mathbf{g}} \rightarrow -\hat{\mathbf{g}} \ . \tag{2.11}$$

Thus each of these irreducible representations $T^{\mathbf{d}}_{M\Lambda}$ that appear in (2.7) is also an eigenstate of $\mathcal{J}$ with an eigenvalue $P=+1$ or -1. The singlet representation **1** is clearly of even parity. As will be shown later in Sec. III, of the three **3** representations (i.e., the three $T^{\mathbf{3}}_{M\Lambda}=D^{1}_{M\Lambda}$ that correspond to the three Λ), two are of $P=-1$ and one of $P=+1$; the same holds for the three $\tilde{\mathbf{3}}$ representations. Two of the **4** representations are of $P=-1$ and the other two of $P=+1$. Of the five **5** representations, two are $P=-1$ and three $P=+1$.

B. Carbon-60

It is useful to separate the six electron wave functions in each C atom into three groups: (i) the two 1*s* inner-core electrons, (ii) the three 2*s*-2*p* valence electrons that link the neighboring carbon atoms in C_{60}, and (iii) the remaining electron, whose *normalized* orbital wave function

$$\chi(\mathbf{r}-\hat{\mathbf{g}}R_0) \tag{2.12}$$

is composed largely of a 2*p* orbit centered around the position vector $\hat{\mathbf{g}}R_0$ of the C nucleus with an azimuthal quantum number $m=0$ along the radial vector $\hat{\mathbf{g}}$ of the unit sphere. In the last category, there are 60 such electrons in C_{60}^{0}, 61 in C_{60}^{-}, etc. These electrons are the ones of importance in our analysis. Let $v(\mathbf{r}-\hat{\mathbf{g}}R_0)$ be the potential generated by one carbon ion C^{+} at $\hat{\mathbf{g}}R_0$ on one of these electrons, at $\mathbf{r}$. The total one-particle Hamiltonian is (in units $\hbar=1$ and mass $=\frac{1}{2}$)

$$\mathcal{H}=-\nabla^2+\sum_g v(\mathbf{r}-\hat{\mathbf{g}}R_0) \ . \tag{2.13}$$

Choose $\chi(\mathbf{r}-\hat{\mathbf{g}}R_0)$ to satisfy

$$[-\nabla^2+v(\mathbf{r}-\hat{\mathbf{g}}R_0)]\chi(\mathbf{r}-\hat{\mathbf{g}}R_0)=\varepsilon_0\chi(\mathbf{r}-\hat{\mathbf{g}}R_0) \tag{2.14}$$

and

$$\int |\chi(\mathbf{r}-\hat{\mathbf{g}}R_0)|^2 d^3r=1 \ . \tag{2.15}$$

In the molecular-orbit approximation,[11] we assume the wave function $\psi(\mathbf{r})$ for C_{60} to be of the form

$$\psi(\mathbf{r})=\sum_g C(g)\chi(\mathbf{r}-\hat{\mathbf{g}}R_0) \ . \tag{2.16}$$

The coefficients $C(g)$ are determined by minimizing the expectation value ε of $\mathcal{H}$:

$$\varepsilon=\frac{\int \psi^*(\mathbf{r})\mathcal{H}\psi(\mathbf{r})d^3r}{\int |\psi(\mathbf{r})|^2 d^3r}=\varepsilon_0+\frac{C^{\dagger}HC}{\int |\psi(\mathbf{r})|^2 d^3r} \ , \tag{2.17}$$

where ψ^* is the complex conjugate of ψ, C is a 60×1 column matrix of components $C(g)$, $C^{\dagger}$ is its Hermitian conjugate, and H is a 60×60 matrix whose matrix elements are

$$\langle g'|H|g\rangle=\tfrac{1}{2}\left[\sum_{g''\neq g'}+\sum_{g''\neq g}\right]\int \chi^*(\mathbf{r}-\hat{\mathbf{g}}'R_0)v(\mathbf{r}-\hat{\mathbf{g}}''R_0)\chi(\mathbf{r}-\hat{\mathbf{g}}R_0)d^3r \ . \tag{2.18}$$

For a short-range potential $v(\mathbf{r}-\hat{\mathbf{g}}R_0)$, the additional tight-binding approximation to the molecular-orbit wave function reduces to

$$C^{\dagger}HC\cong\varepsilon_0'+\varepsilon_1 C^{\dagger}hC \ , \tag{2.19}$$

where $C(g)$ is normalized so that

$$C^{\dagger}C=1 \ ,$$

ε_0' is the diagonal matrix element of H (all diagonal elements of H are identical),

$$\varepsilon_1=\langle g'|H|g\rangle \quad \text{when } (g,g')=\text{nearest neighbors} \ , \tag{2.20}$$

and

$$\langle g'|h|g\rangle=\begin{cases}1 & \text{for } (g,g')=\text{nearest neighbors,}\\ 0 & \text{otherwise}\end{cases} \tag{2.21}$$

is the reduced interaction Hamiltonian. Note that both ε_0' and ε_1 are considered to be small, since each involves the overlapping products of either $\chi(\mathbf{r}-\hat{\mathbf{g}}R_0)$ or $v(\mathbf{r}-\hat{\mathbf{g}}R_0)$ of different neighboring sites. To the same accuracy of smallness, we can approximate the denominator in (2.17) by $C^{\dagger}C=1$; therefore,

$$\varepsilon\cong\varepsilon_0+\varepsilon_0'+\varepsilon_1 C^{\dagger}hC \ ; \tag{2.22}$$

in addition, for χ real and (g,g') nearest neighbors, we may write

$$\varepsilon_1=\int \chi(\mathbf{r}-\hat{\mathbf{g}}'R_0)v(\mathbf{r}-\hat{\mathbf{g}}R_0)\chi(\mathbf{r}-\hat{\mathbf{g}}R_0)d^3r \ . \tag{2.23}$$

In C_{60} each site, say, e, has three nearest-neighboring sites, labeled

$$f_1, \ f_2, \text{ and } f_3 \ , \tag{2.24}$$

as in Fig. 1. (The distance $\overline{ef_2}=\overline{ef_3}$ is slightly different from $\overline{ef_1}$, but we shall treat these three nearest neighbors on an equal basis, as an approximation.) In terms of the regular representation $|\mathbf{d},M,\Lambda\rangle$, we have

$$\langle \mathbf{d},M,\Lambda|h|\mathbf{d}',M',\Lambda'\rangle=\sum_g\sum_{g'}\langle \mathbf{d},M,\Lambda|g\rangle\langle g|h|g'\rangle\langle g'|\mathbf{d}',M',\Lambda'\rangle \ .$$

Because of (2.21) and (2.24), the sum over g' extends only to $g'=gf_a$, with $a=1,2,3$. Let ω_g and ω_f be the Euler angles associated with g and f and ω_{gf} those with the product gf; we have

$$T^{\mathbf{d}}_{M\Lambda}(\omega_{gf})=\sum_N T^{\mathbf{d}}_{MN}(\omega_g)T^{\mathbf{d}}_{N\Lambda}(\omega_f) \ .$$

Hence, by using (2.7) and (2.9), we obtain

$$\langle \mathbf{d},M,\Lambda|h|\mathbf{d}',M',\Lambda'\rangle = \delta_{\mathbf{dd}'}\delta_{MM'}\sum_{a=1}^{3} T^{\mathbf{d}}_{\Lambda\Lambda'}(f_a)\ ; \quad (2.25)$$

to simplify our notation, we write $T^{\mathbf{d}}_{MN}(\omega_f)=T^{\mathbf{d}}_{MN}(f)$. Thus the energy levels of C_{60} are determined by the eigenvalues λ of $\sum_a T^{\mathbf{d}}_{\Lambda\Lambda'}(f_a)$. In all cases it turns out that we need only to diagonalize 2×2 matrices, which can readily be done analytically. The eigenvalues λ of h are given in Table I (see especially its caption and the discussion given in the next section). These values are consistent with those already appearing in the literature.[12,13]

From the resonance energy of benzene,[10] we infer that

$$\varepsilon_1 \sim -1.5 \text{ eV} \quad (2.26)$$

is negative. (There is a fair amount of uncertainty in ε_1 which may vary from -1.5 to about -2.5 eV.) From Table I we see that the lowest-energy level is 1^+, then $3^-,\ldots,$ up to 5^-, which completes the closed shell of 60 electrons. (The superscript $\pm$ denotes the parity.) Above the 60 closed shell, the first excited states form a triplet of negative parity, 3^-, with an excitation energy

$$\varepsilon_- \equiv \varepsilon(3^-)=0.7566|\varepsilon_1|\ ; \quad (2.27)$$

the second excited levels 3^+ form another triplet, but of positive parity with an excitation energy

$$\varepsilon_+ \equiv \varepsilon(3^+)=|\varepsilon_1|\ . \quad (2.28)$$

This is then followed by a quintet 5^+ with an excitation energy

$$\varepsilon(5^+)=1.9208|\varepsilon_1|\ , \quad (2.29)$$

etc. Altogether, there are 120 states, including the spin. Because carbon has positive electronic affinity with the energy of C^- *less* than that of C^0+e^- by about 1.25 eV, the C_{60}^- ion exists in isolation.

As we gradually fill electrons into these molecular orbits, the mean potential "felt" by the successive electrons will be steadily reduced. Apart from this mean average, the overall shape of $v(\mathbf{r}-\hat{\mathbf{g}}R_0)$ is less affected. Even though the values of ε_0' and ε_1 in (2.19) do not really stay constant, but vary slowly depending on the molecular orbits that are already filled, nevertheless the ordering of the states and the relative spacing between nearby levels follow the eigenvalues of the reduced Hamiltonian h, given by (2.25). The ε_1 value in (2.26) refers to those states near the 60 closed shell, but only as an estimate.

TABLE I. Eigenvalues λ of the reduced interaction Hamiltonian h, given by (2.21) and (2.25). Each representation $\mathbf{d}^P$ (with the parity $P=\pm$) has $2d$ levels, including the spin degeneracy. These λ are derived analytically. In closed form, $\lambda=\frac{1}{2}[(3+\sqrt{5})/2\pm\sqrt{(19-\sqrt{5})/2}]$ and $\frac{1}{2}(-3+\sqrt{5})$ for $\mathbf{d}=3$, $\lambda=\frac{1}{2}[(3-\sqrt{5})/2\pm\sqrt{(19+\sqrt{5})/2}]$ and $\frac{1}{2}(-\sqrt{3}-\sqrt{5})$ for $\mathbf{d}=\bar{3}$, $\lambda=1$, -2, and $\frac{1}{2}(-1\pm\sqrt{17})$ for $\mathbf{d}=4$, and $\lambda=1$, $\frac{1}{2}(1\pm\sqrt{13})$, and $\frac{1}{2}(-1\pm\sqrt{5})$ for $\mathbf{d}=5$.

Representation	λ	Representation	λ
1^+	3.0000	3^-	-0.1386
3^-	2.7566	3^+	-0.3820
5^+	2.3028	5^+	-1.3028
$\bar{3}^-$	1.8202	$\bar{3}^-$	-1.4380
4^-	1.5615	5^-	-1.6180
$4^+,5^+$	1.0000	4^+	-2.0000
5^-	0.6180	4^-	-2.5616
		$\bar{3}^+$	-2.6180

It is of interest to attempt an (approximate) identification between the levels in Table I and the spherical harmonics Y_{lm}. We identify the lowest-energy level 1^+ with $l=0$, the second-lowest-energy level 3^- with $l=1$, and the third-lowest-energy level 5^+ with $l=2$. Continuing in the order of increasing energy (i.e., decreasing λ), we identify the next two levels $\bar{3}^-$ and 4^- with $l=3$ [in accordance with the explanation given in the paragraph containing (2.4)–(2.6)] and then the levels 4^+ and 5^+ with $l=4$. This simple monotonic relation between l and λ breaks down near the 60 closed shell for $l=5$ and 6. The highest-occupied molecular-orbital (HOMO) level 5^- and the LUMO level 3^- both correspond only to parts of $l=5$, but the LUMO+1 level 3^+ corresponds to part of $l=6$ (with the remaining part of $l=5$ given by the LUMO+3 level 3^-). In addition, the LUMO 3^- and LUMO+1 3^+ levels are nearly degenerate, as will be explained in the next section.

III. PARITY DOUBLETS

From (2.27) and (2.28), we see that the first two low-lying excitations of C_{60}^-, 3^- and 3^+, are nearly degenerate. Each is a triplet, consisting of 2×3 degenerate states, including spin. Together, 3^- and 3^+ form six pairs of parity doublets. As we shall show, this remarkable feature persists throughout $C_{60}^{2-}, C_{60}^{3-},\ldots,C_{60}^{n-}$, even after we take into account the Coulomb energy between these n electrons (at least for n not too large). As mentioned in the Introduction, the existence of parity doublets makes it possible for us to derive analytic expressions for the essential parts of various strong-interaction effects; this can be achieved by restricting the Hilbert space to one consisting only of the nearby parity doublets. The contributions due to the remaining far-away levels can then be taken into account either numerically or perturbatively.

A. Vector and axial vector near degeneracy

We first examine the diagonalization of the 3×3 matrix

$$\sum_{a=1}^{3} T^{3}_{\Lambda\Lambda'}(f_a)=\sum_{a=1}^{3} D^{1}_{\Lambda\Lambda'}(f_a)\ , \quad (3.1)$$

which, as given by (2.25), forms the reduced Hamiltonian h for $\mathbf{d}=3$ [hence $J=1$ in accordance with (2.8)]; its eigenvectors determine these parity doublets. In Fig. 1 take $\mathbf{ON}$ to be the z axis (in the "laboratory frame"). Let the edge $\overline{A_1N}$ of the icosahedron be on the (x,z) plane. The point e is on $\overline{A_1N}$ with $\hat{\mathbf{e}}\|\mathbf{Oe}$ as before. The unit radial vectors $\hat{\mathbf{f}}_1$, $\hat{\mathbf{f}}_2$, and $\hat{\mathbf{f}}_3$ are associated with the three nearest neighbors f_a of e, with $\hat{\mathbf{f}}_a\|\mathbf{Of_a}$. Let m be the

midpoint of $\overline{A_1N}$. A rotation of a π radian along $\overline{0m}$ takes $\hat{\mathbf{e}}$ to $\hat{\mathbf{f}}_1$. Since

$$\theta \equiv \angle m0N = \frac{1}{2}\cos^{-1}\left[\frac{1}{\sqrt{5}}\right], \tag{3.2}$$

the corresponding matrix $D^1_{\Lambda\Lambda'}(f_1)$ is

$$\begin{bmatrix} -\cos 2\theta & 0 & \sin 2\theta \\ 0 & -1 & 0 \\ \sin 2\theta & 0 & \cos 2\theta \end{bmatrix}. \tag{3.3}$$

The points $\hat{\mathbf{f}}_2$ and $\hat{\mathbf{f}}_3$ can be reached from $\hat{\mathbf{e}}$ through the z-axis rotations of $2\pi/5$ and $-2\pi/5$. Thus the sum $D^1_{\Lambda\Lambda'}(f_2)+D^1_{\Lambda\Lambda'}(f_3)$ gives the matrix

$$\begin{bmatrix} 2\cos(2\pi/5) & 0 & 0 \\ 0 & 2\cos(2\pi/5) & 0 \\ 0 & 0 & 2 \end{bmatrix}. \tag{3.4}$$

The eigenvalues of (3.3)+(3.4) are

$$\lambda_0 = \frac{1}{2}\left[\frac{3+\sqrt{5}}{2} + \left[\frac{19-\sqrt{5}}{2}\right]^{1/2}\right] = 2.7566 ,$$

$$\lambda_- = \frac{1}{2}\left[\frac{3+\sqrt{5}}{2} - \left[\frac{19-\sqrt{5}}{2}\right]^{1/2}\right] = -0.1386 , \tag{3.5}$$

and

$$\lambda_+ = 2\cos\left[\frac{2\pi}{5}\right] - 1 = \frac{1}{2}(-3+\sqrt{5}) = -0.3820 .$$

The corresponding eigenvectors are

$$\hat{\mathbf{e}}_a = \begin{bmatrix} \lambda_a - 2 - \frac{1}{\sqrt{5}} \\ 0 \\ \frac{2}{\sqrt{5}} \end{bmatrix} \left[\left[\lambda_a - 2 - \frac{1}{\sqrt{5}}\right]^2 + \frac{4}{5}\right]^{-1/2}, \tag{3.6}$$

for $a = 0, -$, and

$$\hat{\mathbf{e}}_+ = \begin{bmatrix} 0 \\ 1 \\ 0 \end{bmatrix} = \hat{\mathbf{e}}_0 \times \hat{\mathbf{e}}_- . \tag{3.7}$$

We note that $\hat{\mathbf{e}}_0$ is very close to the radial vector $\hat{\mathbf{e}}$, within

$$\text{an angle} \sim 1^\circ ; \tag{3.8}$$

likewise, $\hat{\mathbf{e}}_-$ is almost parallel to $\overrightarrow{NA}_1$. These three orthonormal unit vectors form the "body-frame" basis vectors at $\hat{\mathbf{e}}$.

From (3.6) and (3.7), by a rigid-body rotation $D^1_{M\Lambda}(g)$, we can obtain the corresponding basis vectors at $\hat{\mathbf{g}}$:

$$\hat{\mathbf{e}}_0(g),\ \hat{\mathbf{e}}_-(g),\ \text{and}\ \hat{\mathbf{e}}_+(g) , \tag{3.9}$$

each a triplet 3. Together, they are the three triplets in the regular representation (2.7). Under the inversion, $\hat{\mathbf{e}} \to -\hat{\mathbf{e}}$; in Fig. 1, the icosahedral vertices $N \to S$, $A_1 \to A_1'$, and consequently $\overrightarrow{NA}_1 \to \overrightarrow{SA}_1' = -\overrightarrow{NA}_1$. The same inversion brings $\hat{\mathbf{g}} \to \hat{\mathbf{g}}_I \equiv -\hat{\mathbf{g}}$, from which we find

$$\hat{\mathbf{e}}_0(g) \to \hat{\mathbf{e}}_0(g_I) = -\hat{\mathbf{e}}_0(g) \tag{3.10a}$$

and

$$\hat{\mathbf{e}}_-(g) \to \hat{\mathbf{e}}_-(g_I) = -\hat{\mathbf{e}}_-(g) ; \tag{3.10b}$$

both are vectors. On the other hand,

$$\hat{\mathbf{e}}_+(g) \to \hat{\mathbf{e}}_+(g_I) = \hat{\mathbf{e}}_0(g_I) \times \hat{\mathbf{e}}_-(g_I) = +\hat{\mathbf{e}}_+(g) , \tag{3.11}$$

which is an axial vector. The levels with the eigenvalue λ_0 lie deep within the 60 closed shell of C_{60}. The orbital wave functions of the first excited levels 3^- are the three components of $\hat{\mathbf{e}}_-(g)$; those of the second excited levels 3^+ are the components of $\hat{\mathbf{e}}_+(g)$. As can be seen from (3.5), the eigenvalues λ_- and λ_+ are quite close to each other.

If we neglect the $\sim 1^\circ$ angle, given by (3.8), the wave function $\hat{\mathbf{e}}_0(g) \cong \hat{\mathbf{g}}$. In contrast, the wave function $\hat{\mathbf{e}}_\pm(g)$ fluctuates a great deal as g varies. For example, according to (3.2) and (3.3), the wave function $\hat{\mathbf{e}}_-(f_1)$ is almost *antiparallel* to $\hat{\mathbf{e}}_-(e)$, even though f_1 and e are nearest neighbors. Since $\hat{\mathbf{e}}_+(g) = \hat{\mathbf{e}}_0(g) \times \hat{\mathbf{e}}_-(g)$, the same applies to the 3^+ wave function. In (2.22), $\varepsilon_1 C^\dagger h C$ serves as the hopping matrix; hence, it is expected that the eigenvalue $\varepsilon_1\lambda_0$ associated with the smooth wave function $\hat{\mathbf{e}}_0(g)$ should be the lowest. Because the magnitudes of variations in $\hat{\mathbf{e}}_+(g)$ and $\hat{\mathbf{e}}_-(g)$ from site to site are similar, their eigenvalues $\varepsilon_1\lambda_+$ and $\varepsilon_1\lambda_-$ become nearly degenerate.

Geometrically, this near degeneracy may also be understood as follows: From (3.2) the angle $\theta = \frac{1}{2}\cos^{-1}(1/\sqrt{5})$ is about 31.7°. In the "planar approximation"

$$\cos\theta = 0.8507 \cong 1 , \tag{3.12}$$

we may regard $\overline{0m} \parallel \overline{0N}$, which is the z axis. Hence the π rotation along $0m$ commutes with the $\pm 2\pi/5$ z axis rotation, and the sum (3.3)+(3.4) becomes a diagonal matrix with its eigenvalue 3 appearing once (corresponding to λ_0) and its other eigenvalue $2\cos(2\pi/5)-1 = -0.3820$ appearing twice (corresponding to λ_- and λ_+); the latter gives the parity doublet.

For small θ the off-diagonal elements in (3.3) are linear in θ; however, for the eigenvalues, the correction to the doublet approximation is only quadratic. Neglecting $O(\theta^4)$, we have

$$\lambda_0 \cong 3 - \frac{2[1-\cos(2\pi/5)]}{2-\cos(2\pi/5)}\theta^2 ,$$
$$\lambda_- \cong 2\cos\left[\frac{2\pi}{5}\right] - 1 + \frac{2[1-\cos(2\pi/5)]}{2-\cos(2\pi/5)}\theta^2 , \tag{3.13}$$

and

$$\lambda_+ = 2\cos\left[\frac{2\pi}{5}\right] - 1 . \tag{3.14}$$

With the quadratic corrections included [for $\theta = \frac{1}{2}\cos^{-1}(1/\sqrt{5})$], $\lambda_0 \cong 2.7496$ and $\lambda_- \cong -0.1316$, which are quite close to their exact values given by (3.5). The λ_+ is already the exact value.

For the diagonalization of h for other irreducible representations, we can follow the same steps by using their explicit wave functions (given in Sec. II). This leads to Table I.

B. Polarizability

The orbital part of the ground-state wave function in C_{60}^- (of the electron outside the 60 closed shell) is

$$\langle g|3^-,i\rangle=\frac{1}{\sqrt{20}}\hat{\mathbf{e}}_-(g)_i \ , \tag{3.15}$$

where $i=x$, y, and z denotes the vector component and the factor $1/\sqrt{20}$ is the normalization constant $\sqrt{d/N}$ in (2.7), with $d=3$ and $N=60$. Likewise, that of its parity doublet is

$$\langle g|3^+,i\rangle=\frac{1}{\sqrt{20}}\hat{\mathbf{e}}_+(g)_i \ . \tag{3.16}$$

The near degeneracy of 3^- and 3^+ makes C_{60}^- highly polarizable. To calculate the polarizability, it is important to isolate the effect of transitions between these two triplets.

In a constant electric field $E\|z$ axis, the interaction (for $E>0$) is

$$-eEz \ . \tag{3.17}$$

To $O(e^2)$ the second-order matrix element is

$$H_{i'i}=-\frac{e^2E^2}{\Delta\varepsilon}\sum_j\langle 3^-,i'|z|3^+,j\rangle\langle 3^+,j|z|3^-,i\rangle \ , \tag{3.18}$$

where, on account of (2.27) and (2.28),

$$\Delta\varepsilon\equiv\varepsilon_+-\varepsilon_-=0.2434|\varepsilon_1| \tag{3.19}$$

is the energy difference between 3^+ and 3^-. From (3.15) and (3.16), it follows that

$$\langle 3^+,j|z|3^-,i\rangle=\tfrac{1}{20}\sum_g\hat{\mathbf{e}}_+(g)_j z(g)\hat{\mathbf{e}}_-(g)_i \ ,$$

which is proportional to ε_{jzi} [$=+1$ (or -1) for $jzi=$even (or odd) permutation of xyz and zero otherwise]. On account of (3.8), if we neglect the 1° difference between $\hat{\mathbf{e}}_0(g)=\hat{\mathbf{e}}_-(g)\times\hat{\mathbf{e}}_+(g)$ and $\hat{\mathbf{g}}$, we find

$$\langle 3^+,j|z|3^-,i\rangle=\tfrac{1}{2}R_0\varepsilon_{jzi} \ , \tag{3.20}$$

where R_0 is the radius of the C_{60}^- ion. The matrix $H_{i'i}$ is diagonal, with

$$H_{xx}=H_{yy}=-\tfrac{1}{2}\alpha E^2 \tag{3.21a}$$

and

$$H_{zz}=0 \ , \tag{3.21b}$$

where

$$\alpha=\frac{1}{2}\frac{e^2R_0^2}{\Delta\varepsilon} \ , \tag{3.22}$$

with $e^2/4\pi\cong 1/137$. Thus, for $i=x$ and y, the polarizability of C_{60}^- is α; for $i=z$, the polarizability is zero. Averaging over these three 3^- orbital states, we have

$$\alpha_{\rm av}=\frac{1}{3}\frac{e^2R_0^2}{\Delta\varepsilon} \ . \tag{3.23}$$

The polarizability of a conducting sphere of radius R_0 is

$$\alpha_c=4\pi R_0^3 \ , \tag{3.24}$$

from which we obtain the ratio

$$\frac{\alpha_{\rm av}}{\alpha_c}=\frac{1}{3}\left[\frac{e^2}{4\pi R_0}\right]\frac{1}{\Delta\varepsilon} \ . \tag{3.25}$$

For $R_0\cong 3.5$ Å and $\varepsilon_1\simeq -1.5$ eV (therefore $\Delta\varepsilon\sim 0.37$ eV), the ratio $\alpha_{\rm av}/\alpha_c$ is ~ 3.6, which is very large. Of course, the estimate (2.26) for ε_1 is rather crude. (But even for $\varepsilon_1\sim -3$ eV, i.e., $\Delta\varepsilon\sim 0.74$ eV, the corresponding ratio $\alpha_{\rm av}/\alpha_c$ is still quite large, ~ 1.8.) We note that, in the C_{60} crystal, the average density ρ is $\cong 1/16R_0^3$; the Clausius-Mossotti limit $\frac{1}{3}\rho\alpha_0=1$ corresponds to a polarizability $\alpha_0=48R_0^3$, which is rather close to the $\alpha_{\rm av}$ of C_{60}^- if $\Delta\varepsilon$ is ~ 0.37 eV.

C. Strong electric field

For a single C_{60}^- ion in a strong electric field $E\|z$ axis, although $|3^\pm,z\rangle$ remains an eigenfunction, the other states $|3^\pm,x\rangle$ and $|3^\pm,y\rangle$ are highly perturbed. Within the reduced Hilbert space defined by these states, one can readily diagonalize the Hamiltonian and find its eigenvalues to be

$$\tfrac{1}{2}(\varepsilon_++\varepsilon_-)\pm\tfrac{1}{2}[(\varepsilon_+-\varepsilon_-)^2+e^2R_0^2E^2]^{1/2} \ . \tag{3.26}$$

When $eR_0E\ll\Delta\varepsilon$, the lower sign gives $\varepsilon_--\frac{1}{2}\alpha E^2$ for the ground-state energy of C_{60}^-. When $eR_0E\gg\Delta\varepsilon$, the ground-state energy becomes $\frac{1}{2}(\varepsilon_++\varepsilon_-)-\frac{1}{2}eR_0E$, which corresponds to a limiting polarization $\frac{1}{2}eR_0$, independent of E.

IV. C_{60}^{2-} ION

A. Wave functions

For a single C_{60}^{2-} ion, we consider a system of two electrons outside the 60 closed shell. The total spin σ can be 0 or 1. In terms of 3^- and 3^+, the total angular momentum l can be 0, 1, or 2; the corresponding *orbital* wave function for the particles at g and g' can be written as

$$\langle g,g'|l,m;p,p'\rangle=\tfrac{1}{20}\sum_{i,i'}C(l,m)_{ii'}\hat{\mathbf{e}}_p(g)_i\hat{\mathbf{e}}_{p'}(g')_{i'} \ , \tag{4.1}$$

where the parity indices p and p' can be $+$ or $-$, m is the z component of the total angular momentum, $C(l,m)_{ii'}$ are coefficients, and as in (3.15) and (3.16), i,i' denote the components of $\hat{\mathbf{e}}_\pm(g)$. It is useful to introduce

$$\Delta_{ii',jj'}(l)\equiv\sum_m C(l,m)^*_{ii'}C(l,m)_{jj'} \ . \tag{4.2}$$

For a normalized wave function (4.1), we have

$$\sum_{i,i',j,j'} \Delta_{ii',jj'}(l)\delta_{ij}\delta_{i'j'}=2l+1 .$$

It can be readily verified that, for $l=0$, 1, and 2,

$$\Delta_{ii',jj'}(0)=\tfrac{1}{3}\delta_{ii'}\delta_{jj'} , \tag{4.3}$$

$$\Delta_{ii',jj'}(1)=\tfrac{1}{2}(\delta_{ij}\delta_{i'j'}-\delta_{ij'}\delta_{ji'}) , \tag{4.4}$$

and

$$\Delta_{ii',jj'}(2)=\tfrac{1}{2}(\delta_{ij}\delta_{i'j'}+\delta_{ij'}\delta_{ji'})-\tfrac{1}{3}\delta_{ii'}\delta_{jj'} . \tag{4.5}$$

The total parity of the wave function is

$$P=pp' . \tag{4.6}$$

Next, we include the dependence on the total spin σ and write the total wave function as the product

$$\langle g,g'|l,m;p,p'\rangle\chi_\sigma , \tag{4.7}$$

where $\chi_\sigma=2^{-1/2}(\uparrow\downarrow'-\downarrow\uparrow')$ for $\sigma=0$ and $\chi_\sigma=\uparrow\uparrow'$ for $\sigma=\sigma_z=1$, etc.

For $P=+$ (i.e., $p=p'=+$ or $-$), introduce

$$^{2\sigma+1}l_{+,\mathrm{sym}}(m)\equiv 2^{-1/2}(\langle g,g'|l,m;+,+\rangle + \langle g,g'|l,m;-,-\rangle)\chi_\sigma \tag{4.8}$$

and

$$^{2\sigma+1}l_{+,\mathrm{asym}}(m)\equiv 2^{-1/2}(\langle g,g'|l,m;+,+\rangle - \langle g,g'|l,m;-,-\rangle)\chi_\sigma . \tag{4.9}$$

The subscripts "sym" and "asym" refer to the symmetry property under the changes $p\rightarrow -p$ and $p'\rightarrow -p'$. Because of Fermi statistics, $l+\sigma$ must be even. Altogether there are $30=2\times(1+3^2+5)$ such states. For $P=-$ (i.e., $p\neq p'$), introduce

$$^{2\sigma+1}l_{-,\mathrm{sym}}(m)\equiv 2^{-1/2}(\langle g,g'|l,m;-,+\rangle + \langle g,g'|l,m;+,-\rangle)\chi_\sigma \tag{4.10}$$

and

$$^{2\sigma+1}l_{-,\mathrm{asym}}(m)\equiv 2^{-1/2}(\langle g,g'|l,m;-,+\rangle - \langle g,g'|l,m;+,-\rangle)\chi_\sigma . \tag{4.11}$$

Here σ can be 0 or 1, for any l [but with $l+\sigma$ even in (4.10) and odd in (4.11)]. Altogether, there are $36=4\times(1+3+5)$ of these states. It is convenient, on the left sides of (4.8)–(4.11), to drop m and to replace l by

$$\mathbf{s},\mathbf{p}, \text{ and } \mathbf{d} , \tag{4.12}$$

for $l=0$, 1, and 2, as in the standard spectroscopic notation. Thus, for example, $^3\mathbf{p}_{+,\mathrm{sym}}$ denotes the $l=1$, $\sigma=1$ symmetrized function given by (4.8), and

$$^1\mathbf{s}_{\pm,\mathrm{sym}} \text{ and } ^1\mathbf{s}_{\pm,\mathrm{asym}} \tag{4.13}$$

refer to the $l=0$, $\sigma=0$, $P=\pm$ symmetrized and antisymmetrized functions.

TABLE II. Sums S_0 and $S_{p_1p_2,p_1'p_2'}$ are defined by (4.21) and (4.19). The exact values of $S_{p_1p_2,p_1'p_2'}$ are calculated by using the $\hat{\mathbf{e}}_\pm(g)$ given by (3.6) and (3.7). Their continuum approximation values are given by (4.41).

	Exact	Continuum approximation
S_0	59.561	$\frac{1}{2}(60+59)=59.50$
$S_{--,--}$	19.197	22
$S_{++,++}$	19.328	22
$S_{--,++}$	5.4147	10
$S_{-+,-+}$	21.946	22
$S_{-+,+-}$	−8.1567	−10
$\frac{1}{2}(S_{--,--}+S_{++,++})$ $-S_{--,++}$	13.848	12
$S_{-+,-+}+S_{-+,+-}$	13.789	12

B. Energy levels

The Coulomb energy between two electrons located at g and g' can be written as

$$V(g,g')=\begin{cases} U_0 & \text{for } g'=g, \\ \dfrac{e^2}{4\pi R_0}\dfrac{1}{|\hat{\mathbf{g}}'-\hat{\mathbf{g}}|} & \text{for } g'\neq g , \end{cases} \tag{4.14}$$

where U_0 is the Coulomb energy when the two electrons are in the same atomic orbit (2.12) and, as before, $R_0\cong 3.5$ Å is the radius of the C_{60} molecule. We estimate

$$U_0\sim 10\text{–}20 \text{ eV} . \tag{4.15}$$

(If we use a hydrogenlike wave function with an effective nuclear charge $Z_{\mathrm{eff}}=3.25$, then $U_0\cong 17.3$ eV.) The Coulomb interaction commutes with the angular momentum and the parity operators. Therefore l, m, and $P=p_1p_2=p_1'p_2'$ are good quantum numbers. The matrix elements of V can be written as

$$\langle l,m';p_1'p_2'|V|l,m;p_1p_2\rangle = \delta_{mm'}\langle p_1'p_2'|V(l)|p_1p_2\rangle . \tag{4.16}$$

By using (4.1)–(4.5) and the orthonormality relation

$$\tfrac{1}{20}\sum_g \hat{\mathbf{e}}_p(g)_i\hat{\mathbf{e}}_{p'}(g)_{i'}=\delta_{pp'}\delta_{ii'} , \tag{4.17}$$

we find, for $l=0$,

$$\langle p_1'p_2'|V(0)|p_1p_2\rangle=\frac{1}{20}\left[U_0\delta_{p_1p_2}\delta_{p_1'p_2'}+\frac{e^2}{4\pi R}S_{p_1p_2,p_1'p_2'}\right] , \tag{4.18}$$

where

$$S_{p_1p_2,p_1'p_2'}=(R/R_0)\sum_{g\neq e}|\hat{\mathbf{e}}-\hat{\mathbf{g}}|^{-1}[\hat{\mathbf{e}}_{p_1}(e)\cdot\hat{\mathbf{e}}_{p_2}(g)][\hat{\mathbf{e}}_{p_1'}(e)\cdot\hat{\mathbf{e}}_{p_2'}(g)]\ , \tag{4.19}$$

R/R_0 is given by (2.2), and the sum extends over all $\hat{\mathbf{g}}\neq\hat{\mathbf{e}}$. Likewise, for $l=1$,

$$(p_1'p_1'|V(1)|p_1p_2)=\frac{1}{40}\left[U_0(\delta_{p_1p_1'}\delta_{p_2p_2'}-\delta_{p_1p_2'}\delta_{p_2p_1'})+\frac{e^2}{4\pi R}(S_0\delta_{p_1p_1'}\delta_{p_2p_2'}-S_{p_1p_2',p_1'p_2})\right]\ , \tag{4.20}$$

where

$$S_0=(R/R_0)\sum_{g\neq e}|\hat{\mathbf{e}}-\hat{\mathbf{g}}|^{-1}=59.56 \tag{4.21}$$

and, for $l=2$,

$$(p_1'p_2'|V(2)|p_1p_2)=\frac{3}{100}\left[U_0\left[\frac{1}{2}\delta_{p_1p_1'}\delta_{p_2p_2'}+\frac{1}{2}\delta_{p_1p_2'}\delta_{p_2p_1'}-\frac{1}{3}\delta_{p_1p_2}\delta_{p_1'p_2'}\right]+\frac{e^2}{4\pi R}\left[\frac{1}{2}S_0\delta_{p_1p_1'}\delta_{p_2p_2'}+\frac{1}{2}S_{p_1p_2',p_1'p_2}-\frac{1}{3}S_{p_1p_2,p_1'p_2'}\right]\right]\ . \tag{4.22}$$

$S_{p_1p_2,p_1'p_2'}$ can be calculated by using $\hat{\mathbf{e}}_{\pm}(g)$ given by (3.6) and (3.7); the results are listed in Table II.

For $l=0$, $\sigma=0$, and $P=+$, we have two states

$$(p,p')=(-,-)\ \text{ and }\ (+,+)\ . \tag{4.23}$$

Their energies, in the absence of the Coulomb interaction, are $2\varepsilon_-$ and $2\varepsilon_+$. Including the Coulomb energy and restricting the Hilbert space to one defined by the two states in (4.23), we can diagonalize the 2×2 Hamiltonian matrix. Its eigenvalues are

$$E_{\pm}=\varepsilon_++\varepsilon_-+\frac{1}{40}\left[2U_0+\frac{e^2}{4\pi R}(S_{--,--}+S_{++,++})\right]\pm\left\{\left[\frac{1}{20}\left[U_0+\frac{e^2}{4\pi R}S_{--,++}\right]\right]^2+\left[\varepsilon_--\varepsilon_++\frac{1}{20}\frac{e^2}{4\pi R}(S_{--,--}-S_{++,++})\right]^2\right\}^{1/2}\ . \tag{4.24}$$

If we neglect the difference $\varepsilon_--\varepsilon_+$, then in accordance with (4.13) the corresponding wave functions are ${}^1\mathbf{s}_{+,\text{sym}}$ for the upper sign and ${}^1\mathbf{s}_{+,\text{asym}}$ for the lower sign. (Later on, for notational convenience, these eigenstates will be simply *designated* as ${}^1\mathbf{s}_{+,\text{sym}}$ and ${}^1\mathbf{s}_{+,\text{asym}}$.)

For $l=0$, $\sigma=0$, but $P=-$, there is only one $2e$ wave function:

$${}^1\mathbf{s}_{-,\text{sym}}=2^{-1/2}(\langle g,g'|0,0;-,+\rangle+\langle g,g'|0,0;+,-\rangle)\chi_0\ . \tag{4.25}$$

Its energy is

$$E_0=\varepsilon_++\varepsilon_-+\frac{1}{20}\frac{e^2}{4\pi R}(S_{-+,-+}+S_{-+,+-})\ . \tag{4.26}$$

In accordance with (2.2) and (2.26), setting $R=4.03$ Å, $\varepsilon_1=-1.5$ eV (i.e., $\varepsilon_-=1.135$ eV and $\varepsilon_+=1.5$ eV), and $U_0=20$ eV, we find $E_-=5.0698$ eV and $E_0=5.0974$ eV, giving a parity doublet, much closer than ε_- and ε_+.

These parity-doublet states

$${}^1\mathbf{s}_{+,\text{asym}}\ \text{ and }\ {}^1\mathbf{s}_{-,\text{sym}} \tag{4.27}$$

are the lowest-energy levels of C_{60}^{2-}. Both have $\sigma=0$, in violation of Hund's rule. This is because, when $g=g'$, we have

$$\hat{\mathbf{e}}_-(g)\cdot\hat{\mathbf{e}}_+(g')+\hat{\mathbf{e}}_+(g)\cdot\hat{\mathbf{e}}_-(g')=0 \tag{4.28a}$$

and

TABLE III. Energy levels of C_{60}^{2-}. The numbers listed correspond to $\Delta\varepsilon=0.37$ eV and $U_0=20$ eV.

Wave function	Multiplicity	Exact energy (eV)	Continuum approximation
${}^1\mathbf{s}_{+,\text{asym}}$	1	5.071	4.777
${}^1\mathbf{s}_{-,\text{sym}}$	1	5.096	4.777
${}^3\mathbf{p}_{+,\text{asym}}$	9	5.420	5.134
${}^3\mathbf{p}_{-,\text{sym}}$	9	5.509	5.134
${}^3\mathbf{d}_{-,\text{asym}}$	15	5.636	5.348
${}^1\mathbf{d}_{+,\text{sym}}$	5	5.661	5.548
${}^3\mathbf{p}_{+,\text{sym}}$	9	7.044	6.919
${}^1\mathbf{d}_{-,\text{sym}}$	5	7.398	7.733
${}^1\mathbf{p}_{-,\text{sym}}$	3	7.476	7.919
${}^1\mathbf{d}_{+,\text{asym}}$	5	7.476	7.733
${}^3\mathbf{s}_{-,\text{asym}}$	3	8.009	8.347
${}^1\mathbf{s}_{+,\text{sym}}$	1	9.076	10.347

$$\hat{\mathbf{e}}_-(g)\cdot\hat{\mathbf{e}}_-(g')-\hat{\mathbf{e}}_+(g)\cdot\hat{\mathbf{e}}_+(g')=0\ ; \tag{4.28b}$$

by having the two electrons thus correlated, it is possible for these wave functions, though symmetric in g and g', to avoid the very large Coulomb repulsion at close distances.

The same method can be readily extended to the excited levels of C_{60}^{2-}. The results are listed in Table III.

C. Comments on the perturbation series in U_0

Recently, Chakravarty, Gelfand, and Kivelson[8] proposed an interesting pairing mechanism based on the perturbation formula in U_0. Our model can provide some insight into the reliability of such a method. In their approach, all off-site ($g\neq g'$) Coulomb interactions are neglected; hence, $S_{p_1p_2,p_1'p_2'}=0$. The ground-state energy (4.24) for C_{60}^{2-} becomes

$$E_-=\varepsilon_++\varepsilon_-+\frac{U_0}{20}-\left[\left[\frac{U_0}{20}\right]^2+(\varepsilon_+-\varepsilon_-)^2\right]^{1/2}. \tag{4.29}$$

The corresponding energy difference between $C_{60}^-+C_{60}^-$ and $C_{60}^{2-}+C_{60}^0$ in our model is

$$\begin{aligned}2E_1-E_2&\equiv 2\varepsilon_--E_-\\&=\varepsilon_--\varepsilon_+-\frac{U_0}{20}+\left[\left[\frac{U_0}{20}\right]^2+(\varepsilon_+-\varepsilon_-)^2\right]^{1/2},\end{aligned} \tag{4.30}$$

which is always negative. On the other hand, to $O(U_0^2)$, the perturbation expansion is

$$2E_1-E_2\cong-\frac{U_0}{20}+\frac{1}{2(\varepsilon_+-\varepsilon_-)}\left[\frac{U_0}{20}\right]^2; \tag{4.31}$$

it becomes positive for

$$\frac{U_0}{20}>2(\varepsilon_+-\varepsilon_-) \tag{4.32}$$

and is misleading. If, as in (2.26), $\varepsilon_1\sim-1.5$ eV, $\varepsilon_+-\varepsilon_-\sim0.37$ eV, then the second-order perturbation gives unreliable results for $U_0>15$ eV.

Chakravarty, Gelfand, and Kivelson give for $2E_1-E_2$, in place of (4.31),

$$-\frac{U_0}{20}+0.0154\frac{U_0^2}{t}, \tag{4.33}$$

where t is $\cong2$–3 eV (and for the case when their parameter x is set to zero). Their calculation includes the effect of all levels, but only up to U_0^2, whereas our formula (4.30) is valid to all orders of U_0, but is derived on the basis of the parity-doublet approximation. Thus a direct comparison is difficult. However, since the ratio $t/(-\varepsilon_1)$ is >1, one sees that from (4.31) the parity doublet contributes in the second-order perturbation

$$\frac{U_0^2}{800}\left[\frac{1}{0.25}\right]\frac{1}{|\varepsilon_1|}>0.005\frac{U_0^2}{t},$$

accounting for at least $\frac{1}{3}$ of the coefficient 0.0154 in (4.33). This does raise the question of whether or not such a second-order perturbation formula can be meaningfully applied to large U_0.

D. Continuum approximation

From Table II we see that the near equality

$$S_{--,--}\cong S_{++,++} \tag{4.34}$$

holds to within 0.7% and

$$\begin{aligned}\tfrac{1}{2}(S_{--,--}+S_{++,++})-S_{--,++}&\\\cong S_{-+,-+}+S_{-+,+-}&\end{aligned} \tag{4.35}$$

to within 0.5%. These two near equalities and the near degeneracy of ε_+ and ε_- (in C_{60}^-) give rise to the parity doublets in C_{60}^{2-}. (Note that with (4.34) the relevant small parameter in (4.24) is the ratio

$$(\varepsilon_+-\varepsilon_-)^2\Big/\left[\frac{1}{20}\left[U_0+\frac{e^2}{4\pi R}S_{--,++}\right]\right]^2,$$

which is $\leq1\%$. Neglecting that, (4.35) leads to $E_-\cong E_0$.) The near identities (4.34) and (4.35) can be understood by applying the following continuum approximation.

We approximate $\hat{\mathbf{e}}_-(g)$ and $\hat{\mathbf{e}}_+(g)$ of (3.6) and (3.7) simply by the first two column matrices (i.e., $\Lambda=1$ and 2) of $D^1_{M\Lambda}(\alpha,\beta,\gamma)$ with α,β,γ as the Euler angles associated with g. In terms of the unit basis vectors $\hat{\mathbf{x}}$, $\hat{\mathbf{y}}$, and $\hat{\mathbf{z}}$ in the laboratory frame, we write

$$\begin{aligned}\hat{\mathbf{e}}_-(g)=&\hat{\mathbf{x}}(\cos\beta\cos\alpha\cos\gamma-\sin\alpha\sin\gamma)\\&+\hat{\mathbf{y}}(\cos\beta\sin\alpha\cos\gamma+\cos\alpha\sin\gamma)\\&-\hat{\mathbf{z}}\sin\beta\cos\gamma\end{aligned} \tag{4.36a}$$

and

$$\begin{aligned}\hat{\mathbf{e}}_+(g)=&-\hat{\mathbf{x}}(\cos\beta\cos\alpha\sin\gamma+\sin\alpha\cos\gamma)\\&-\hat{\mathbf{y}}(\cos\beta\sin\alpha\sin\gamma-\cos\alpha\cos\gamma)\\&+\hat{\mathbf{z}}\sin\beta\sin\gamma,\end{aligned} \tag{4.36b}$$

with the integral

$$\int_0^{\pi}\sin\beta\,d\beta\int_0^{2\pi}d\alpha\int_0^{2\pi}d\gamma=8\pi^2, \tag{4.37}$$

replacing the sum over either

$$\sum_g 1=60 \tag{4.38a}$$

or

$$\sum_{g\neq e}1=59\ . \tag{4.38b}$$

This ambiguity makes us approximate the exact $S_0=59.56$ by

$$S_0=\frac{1}{2}(60+59)\int\frac{1}{8\pi^2}\sin\beta\,d\beta\,d\alpha\,d\gamma\left[2\sin\frac{\beta}{2}\right]^{-1}$$
$$=59.50\ , \tag{4.39}$$

in which we take $\hat{\mathbf{e}}=\hat{\mathbf{z}}$,

$$\hat{\mathbf{g}}=\hat{\mathbf{e}}_-(g)\times\hat{\mathbf{e}}_+(g)$$
$$=\hat{\mathbf{x}}\sin\beta\cos\alpha+\hat{\mathbf{y}}\sin\beta\sin\alpha+\hat{\mathbf{z}}\cos\beta\ , \tag{4.40}$$

and therefore $|\hat{\mathbf{e}}-\hat{\mathbf{g}}|=2\sin(\beta/2)$. (In addition, we neglect the small difference between the C_{60} radius R_0 and the circumspherical radius R of the icosahedron in Fig. 1.)

For simplicity, we use the measure (4.37) to replace the sum $\sum_g 1=60$ in the following. Setting $\hat{\mathbf{e}}_-(e)=\hat{\mathbf{x}}$ and $\hat{\mathbf{e}}_+(e)=\hat{\mathbf{y}}$, we derive the following continuum approximations for $S_{p_1p_2,p_1'p_2'}$:

$$S_{--,--}=S_{++,++}=S_{-+,-+}=22 \tag{4.41a}$$

and

$$S_{--,++}=-S_{-+,+-}=10\ , \tag{4.41b}$$

which account for (4.34) and (4.35). Comparisons with the exact values are given in Table II. As mentioned in Sec. III A, $\hat{\mathbf{e}}_\pm(g)$ can vary a great deal from g to neighboring g'. In the continuum approximation, the γ dependence in (4.36) reflects this fluctuation. [The exact $S_{p_1p_2,p_1'p_2'}$ satisfy (4.34) and (4.35) much more closely than one might expect from the rough accuracy of the continuum approximation; this is because (4.34) and (4.35) are also true in the "planar approximation," in which each $\hat{\mathbf{g}}=\hat{\mathbf{e}}_-(g)\times\hat{\mathbf{e}}_+(g)$ is taken to be equal to $\hat{\mathbf{e}}$. These two approximations complement each other for short- and long-range interactions.]

In the following we apply only the continuum approximation, but together with the approximate equality $\varepsilon_+=\varepsilon_-$; this leads to the energy for the singlet, $l=0$, $P=+$ level,

$$E(^1\mathbf{s}_{+,\mathrm{asym}})=2\bar{\varepsilon}+\frac{1}{20}\frac{e^2}{4\pi R}\left[\frac{1}{2}(S_{--,--}+S_{++,++})-S_{--,++}\right]\ , \tag{4.42}$$

and that for the singlet, $l=0$, $P=-$ level,

$$E(^1\mathbf{s}_{-,\mathrm{sym}})=2\bar{\varepsilon}+\frac{1}{20}\frac{e^2}{4\pi R}(S_{-+,-+}+S_{-+,+-})\ , \tag{4.43}$$

where

$$\bar{\varepsilon}=\tfrac{1}{2}(\varepsilon_++\varepsilon_-)\ . \tag{4.44}$$

These two energies are the same on account of (4.41).

The next levels are $^3\mathbf{p}_{+,\mathrm{asym}}$ and $^3\mathbf{p}_{-,\mathrm{sym}}$ with the same energy

$$2\bar{\varepsilon}+\frac{7}{10}\frac{e^2}{4\pi R}\ , \tag{4.45}$$

followed by $^3\mathbf{d}_{-,\mathrm{asym}}$ of energy

$$2\bar{\varepsilon}+\frac{19}{25}\frac{e^2}{4\pi R}\ , \tag{4.46}$$

and then by $^1\mathbf{d}_{+,\mathrm{sym}}$ of energy

$$2\bar{\varepsilon}+\frac{U_0}{100}+\frac{19}{25}\frac{e^2}{4\pi R}\ , \tag{4.47}$$

by $^3\mathbf{p}_{+,\mathrm{sym}}$ of energy

$$2\bar{\varepsilon}+\frac{6}{5}\frac{e^2}{4\pi R}\ , \tag{4.48}$$

and by $^1\mathbf{p}_{-,\mathrm{asym}}$ of energy

$$2\bar{\varepsilon}+\frac{U_0}{20}+\frac{6}{5}\frac{e^2}{4\pi R}\ . \tag{4.49}$$

After these, $^1\mathbf{d}_{+,\mathrm{asym}}$ and $^1\mathbf{d}_{-,\mathrm{sym}}$ form another set of parity doublets with energy

$$2\bar{\varepsilon}+\frac{3U_0}{100}+\frac{63}{50}\frac{e^2}{4\pi R}\ , \tag{4.50}$$

then followed by $^3\mathbf{s}_{-,\mathrm{asym}}$ of energy

$$2\bar{\varepsilon}+\frac{8}{5}\frac{e^2}{4\pi R}\ , \tag{4.51}$$

and by $^1\mathbf{s}_{+,\mathrm{sym}}$ of energy

$$2\bar{\varepsilon}+\frac{U_0}{10}+\frac{8}{5}\frac{e^2}{4\pi R}\ . \tag{4.52}$$

Table III compares these approximate values with the exact energies.

For $R\simeq 4$ Å, $e^2/4\pi R$ is $\cong 3.6$ eV. We expect U_0 to be not larger than 20 eV; in that case, these energies are dominated by the off-site Coulomb interaction ($g\neq g'$) in (4.14).

V. MADELUNG ENERGY

In the preceding sections, we examined the physical properties of C_{60}^- and C_{60}^{2-} in isolation. However, our main interest is to study the K_nC_{60} crystal. In this section we turn to the question whether all K atoms are positively ionized.

Take K_3C_{60}. The C_{60} molecules form a face-centered-cubic lattice.[14] Its Wigner-Seitz (or Voronoi) cell is a rhombic dodecahedron, one that has 12 identical faces, each a parallelogram with four equal edges (altogether 24 edges). The center of the dodecahedron is C_{60}, and each of its 14 vertices is occupied by one K atom. Six of the K vertices are at a distance

$$\tfrac{1}{2}l \cong 7.1 \text{ Å} \tag{5.1}$$

from C_{60}; these may be called "octahedral vertices," since by themselves they form a regular octahedron. The remaining eight K vertices are all at $(\sqrt{3}/4)l \cong 6.15$ Å from C_{60}. Each of the six octahedral vertices is shared by six C_{60} molecules and each of the remaining eight by four C_{60} molecules, making a total of three K atoms for each C_{60} molecule.

The Madelung energy E_M of $K_3^+C_{60}^{3-}$ per each C_{60} molecule can readily be calculated (see the Appendix). The result is

$$E_M(K_3C_{60}) = \frac{3e^2}{2l}(-1+2\kappa) , \tag{5.2}$$

$$\kappa = -2\sum_{m_1 m_2} \frac{1}{\cosh^2 \pi m'} + \sum_{m_1 m_2}{}' \frac{1-(-)^{m_1+m_2}\cosh \pi m}{\sinh^2 \pi m} , \tag{5.3}$$

where $m = (m_1^2 + m_2^2)^{1/2}$, $m' = [(m_1+\frac{1}{2})^2 + (m_2+\frac{1}{2})^2]^{1/2}$, the sums $\sum_{m_1 m_2}$ and $\sum'_{m_1 m_2}$ are both over all integral values of m_1 and m_2, except $m_1 = m_2 = 0$ is excluded in $\sum'_{m_1 m_2}$; numerically,

$$E_M(K_3C_{60}) = -22.12\frac{e^2}{4\pi l} \cong -22.41 \text{ eV} . \tag{5.4}$$

For an isolated K atom, the ionization energy is

$$E(K^+ + e) - E(K^0) \cong 4.34 \text{ eV} \tag{5.5}$$

and, for a C atom,

$$E(C^-) - E(C^0 + e) \cong -1.25 \text{ eV} . \tag{5.6}$$

Since the sum (5.4)+3[(5.5)+(5.6)] is −13.14 eV, we expect all the K atoms in K_3C_{60} to be ionized. [Besides (5.4)–(5.6), there are other energies, such as the mutual Coulomb energy between the three e, their kinetic energy, etc., as will be considered in the next section; however, the very large Madelung energy remains the dominant factor.]

An upper bound on the Madelung energy of K_1C_{60} or K_2C_{60} can be derived by placing the K^+ ions on all the octahedral vertices for K_1C_{60}, but only on the nonoctahedral vertices for K_2C_{60}. We find that, per C_{60} molecule, the upper bound for $K_1^+C_{60}^-$ is

$$E_M(K_1C_{60}) \leq -3.54 \text{ eV} , \tag{5.7}$$

which is lower than the sum (5.5)+(5.6) by only −0.46 eV, indicating perhaps that the K atoms are also ionized. The corresponding upper bound for the Madelung energy of $K_2^+C_{60}^{2-}$ is

$$E_M(K_2C_{60}) \leq -11.79 \text{ eV} , \tag{5.8}$$

which is much lower than 2 times (5.5)+(5.6), giving the conclusion that all K atoms are ionized.

Unlike K_3C_{60}, the K sites in K_1C_{60} and K_2C_{60} can easily be perturbed. By varying these K sites, one can reach many other configurations with comparably low (or lower) Madelung energy. This may be the reason why neither K_1C_{60} nor K_2C_{60} has yet shown a clear crystal structure.

Another interesting question is to examine the change in Madelung energy due to charge fluctuations. Decompose the face-centered-cubic lattice of C_{60} into alternate even and odd layers of two-dimensional $d \times d$ square lattices, with $d = l/\sqrt{2}$. Let the z axis be perpendicular to these layers. The lattice sites on the even layers are located at $(x,y) = (n_1 d, n_2 d)$ and those on the odd layers at $((n_1+\frac{1}{2})d, (n_2+\frac{1}{2})d)$, with n_1 and n_2 integers. Along the z axis, the separation between two neighboring even and odd layers is $l/2$. Consider a charge fluctuation in which every C_{60} molecule on the even layers carries a fluctuation charge $+q$ and on the odd layers $-q$. Then, in addition to the average Madelung energy calculated before, there is a fluctuation Madelung energy F_M per C_{60}:

$$F_M = \frac{q^2}{4\pi\sqrt{2}l}\left[-\frac{4\pi}{3} + \frac{\pi}{\sqrt{2}} + c\right] , \tag{5.9}$$

where

$$c = \sum_{m_1 m_2}{}' \left[\frac{3\pi}{\sinh^2 \pi m} - \frac{e^{-\pi m}}{m \sinh \pi m} + \frac{e^{-\sqrt{2}\pi m} - (-1)^{m_1+m_2}}{m \sinh \sqrt{2}\pi m}\right] = 0.3730 . \tag{5.10}$$

Numerically,

$$F_M \cong -1.127\frac{q^2}{4\pi l} < 0 . \tag{5.11}$$

Setting $l \cong 14.2$ Å and $q = e$, we find $F_M \cong -1.14$ eV. Thus the Madelung energy favors charge fluctuations[15] between neighboring C_{60} layers, similar to CuO_2 layers in Y 1:2:3 and Tl 2:2:2:3.

Of course, such charge fluctuations will raise the Coulomb energy within each Wigner-Seitz cell; in addition, because these are highly correlated fluctuations, there would be an increase in kinetic energy. These increases are partly offset by the negative Madelung energy.

VI. FERMIONS VS BOSONS

A. Pairing mechanism

Above the 60 closed shell, a typical band calculation[16] for K_nC_{60} reveals a low-lying cluster of three overlapping narrow bands, which is the Bloch wave extension of the three 3^- orbital levels of an isolated C_{60}. In the tight-binding limit, the corresponding one-particle Bloch wave function of wave number vector $\mathbf{k}$ can be written as

$$\frac{1}{\sqrt{\mathcal{N}}}\sum_a e^{i\mathbf{k}\cdot\mathbf{R}_a}\psi(\mathbf{r}-\mathbf{R}_a) . \tag{6.1}$$

The sum goes over all lattice-site positions $\mathbf{R}_a$ of C_{60}, $\mathcal{N}$ is the total number of lattice sites, and $\psi(\mathbf{r}-\mathbf{R}_a)$ is the

molecular-orbit wave function (2.16):

$$\psi(\mathbf{r}-\mathbf{R}_a)=\sum_{g,i} C_i(\mathbf{k})\langle g|3^-,i\rangle\chi(\mathbf{r}-\hat{\mathbf{g}}R_0-\mathbf{R}_a)\ , \tag{6.2}$$

where $\langle g|3^-,i\rangle=\hat{\mathbf{e}}_-(g)_i/\sqrt{20}$ is given by (3.15) and $\chi(\mathbf{r}-\hat{\mathbf{g}}R_0-\mathbf{R}_a)$ is the same function in (2.12). The vector $\mathbf{k}$ breaks the threefold degeneracy of 3^- (in an isolated C_{60} molecule); the coefficients $C_i(\mathbf{k})$, with $i=x,y,z$, are determined by minimizing the energy.

Above this cluster of three narrow bands (in the order of energy excitations), there is a second cluster of three overlapping narrow bands, corresponding to the Bloch wave extension of the three 3^+ levels. These two clusters are separated by an energy gap $\cong\Delta\varepsilon=\varepsilon_+-\varepsilon_-$. Label the first cluster the "3^- band" and the second the "3^+ band." In such a band calculation, for K_nC_{60} with $n\le 6$, the ground-state electrons (not counting the core ones) are all in the 3^- band.

Instead of the one-particle Bloch wave function (6.1), there is a different possibility. We may consider the Bloch extension of a correlated two-particle function at positions $\mathbf{r}$ and $\mathbf{r}'$:

$$\frac{1}{\sqrt{\mathcal{N}}}\sum_a e^{i\mathbf{k}\cdot\mathbf{R}_a}\sum_{g,g'}\langle g,g'|{}^1\mathbf{s}_{-,\mathrm{sym}}\rangle\chi(\mathbf{r}-\hat{\mathbf{g}}R_0-\mathbf{R}_a)\chi(\mathbf{r}'-\hat{\mathbf{g}}'R_0-\mathbf{R}_a)\ , \tag{6.3}$$

where $\langle g,g'|{}^1\mathbf{s}_{-,\mathrm{sym}}\rangle$ is the right-hand side of (4.25). In terms of $\hat{\mathbf{e}}_\pm(g)$ given by (3.6) and (3.7), we have

$$\langle g,g'|{}^1\mathbf{s}_{-,\mathrm{sym}}\rangle = \frac{1}{20\sqrt{6}}[\hat{\mathbf{e}}_-(g)\cdot\hat{\mathbf{e}}_+(g')+\hat{\mathbf{e}}_+(g)\cdot\hat{\mathbf{e}}_-(g')]\chi_0 \tag{6.4a}$$

and

$$\chi_0=\frac{1}{\sqrt{2}}(\uparrow\downarrow'-\downarrow\uparrow')\ . \tag{6.4b}$$

Because

$$\sum_g \hat{\mathbf{e}}_-(g)_i\hat{\mathbf{e}}_+(g)_j=0\ , \tag{6.5}$$

this correlated two-particle wave function (6.3) is *orthogonal* to any product of two one-particle wave functions in the 3^- band. In the following we call the band constructed out of (6.3) the "boson band" and the correlated two-electron wave function ${}^1\mathbf{s}_{-,\mathrm{sym}}$ a "boson," which is a pseudoscalar. The small hopping transition amplitude of bosons makes the boson band much narrower than the 3^-, or 3^+, band. (The boson band studied in this section is the "pseudoscalar band." Note that had we used the scalar ${}^1\mathbf{s}_{+,\mathrm{asym}}$, we would not have the orthogonality relation with the 3^- band; whether such a "scalar band" can exist or not will be discussed in Sec. VIII.)

Two electrons in the 3^- band have an energy advantage over the boson on account of the excitation energy $\Delta\varepsilon=\varepsilon_+-\varepsilon_-$ and the lowering in kinetic energy; however, there is a disadvantage to the 3^- band by having a higher Coulomb energy. The important question concerning the roles of bosons versus fermions depends on the delicate balance between these opposing factors.

At the symmetry point Γ (i.e., $\mathbf{k}=0$) in the band calculation, the three 3^- bands become degenerate and the same holds for the three 3^+ bands; the energy separation between the 3^- and 3^+ bands at Γ, obtained by Xu, Huang, and Ching,[16] is quite near the value

$$\Delta\varepsilon=\varepsilon_+-\varepsilon_-\cong 0.37\ \mathrm{eV}\ , \tag{6.6}$$

given by (2.26)–(2.28), for $\varepsilon_1\cong -1.5$ eV. The energy difference K between Γ and the bottom of the 3^- band gives an estimate of the lowering of the kinetic energy of each electron due to the hopping degrees of freedom of the electrons. From the band calculation,[16] for one e,

$$K\cong 0.4\ \mathrm{eV}\ . \tag{6.7}$$

The sum $\Delta\varepsilon+2K\cong 1.17$ eV is in favor of the two e in the 3^- band over the boson band. As we shall see, the difference in their Coulomb energies gives a preference in the other direction.

B. Coulomb energy between uncorrelated 3^- electrons

In the following we will give only model calculations which (we hope) may exhibit qualitatively the essential features of the physical situation. We separate the Coulomb-energy problem into two general categories: (i) the energy within one Wigner-Seitz cell (but excluding that between K_n^+ and C_{60}^{n-}) and (ii) the rest (including the Madelung energy, already calculated in Sec. V). In this section we shall only examine (i). For the electrons in the 3^- band, we make the approximation that their Coulomb energy in case (i) corresponds to that between uncorrelated 3^- electrons in the same C_{60} molecule.

We recall that in a single C_{60} molecule, including the spin, there are altogether 2×3 states in 3^-. For two e, both in 3^-, there are six states if the total spin $\sigma=0$ and nine states if $\sigma=1$. Assume these two electrons to be uncorrelated; i.e., they can be in any of these $15=6+9$ states with an equal probability. By using (4.18)–(4.22) and setting $p_1=p_2=p_1'=p_2'=-$, we find that the average Coulomb energy (4.14) between such a pair of electrons is

$$\varepsilon_{\mathrm{pair}}=\frac{1}{100}\left[U_0+\frac{e^2}{4\pi R}(2S_0-S_{--,--})\right]\ . \tag{6.8}$$

For n such uncorrelated electrons (but in a completely antisymmetrized wave function), the corresponding average Coulomb energy is, for $n\le 6$,

$$\varepsilon(ne)_{\mathrm{Coul}}=\tfrac{1}{2}n(n-1)\varepsilon_{\mathrm{pair}}\ . \tag{6.9}$$

Next, we consider a system of one "boson" and m uncorrelated 3^- electrons, all confined to the same C_{60} molecule; i.e., the system has $n=2+m$ electrons with two electrons in ${}^1\mathbf{s}_{-,\mathrm{sym}}$ and the other m uncorrelated 3^-

electrons. [We first write down such a product wave function and then sum over all its permutations $\mathcal{P}$ and multiply each term by $(-)^{\mathcal{P}}$.] The resulting average Coulomb energy is

$$\varepsilon(b+me)_{\rm Coul}=\varepsilon(b)_{\rm Coul}+2m\varepsilon'_{\rm pair}+\tfrac{1}{2}m(m-1)\varepsilon_{\rm pair}\ , \tag{6.10}$$

where, on account of (4.26),

$$(\varepsilon_b)_{\rm Coul}=\frac{1}{20}\frac{e^2}{4\pi R}(S_{-+,-+}+S_{-+,+-}) \tag{6.11}$$

denotes the Coulomb energy between the $2e$ in the boson, $\varepsilon_{\rm pair}$ is given by (6.8), and

$$\varepsilon'_{\rm pair}=\frac{1}{100}\left\{U_0+\frac{e^2}{4\pi R}\left[2S_0-\frac{1}{2}(S_{--,--}+S_{--,++}+S_{-+,-+}+S_{-+,+-})\right]\right\} \tag{6.12}$$

is $\frac{1}{2}$ times the Coulomb energy between one of the m uncorrelated e and the boson. From Table II and because of (4.34) and (4.35), we see that the difference

$$\varepsilon'_{\rm pair}-\varepsilon_{\rm pair}=\frac{1}{200}\frac{e^2}{4\pi R}(S_{--,--}-S_{--,++}-S_{-+,-+}-S_{-+,+-}) \tag{6.13}$$

is nearly zero; the equality

$$\varepsilon'_{\rm pair}=\varepsilon_{\rm pair} \tag{6.14}$$

holds to within 0.1%. Therefore, for $n=2+m$,

$$\varepsilon(ne)_{\rm Coul}-\varepsilon(b+me)_{\rm Coul}\cong\varepsilon(2e)_{\rm Coul}-\varepsilon(b)_{\rm Coul}=\frac{1}{100}\left\{U_0+\frac{e^2}{4\pi R}[2S_0-S_{--,--}-5(S_{-+,-+}+S_{-+,+-})]\right\}\ , \tag{6.15}$$

independent of m. Take the C_{60} radius $R_0\cong 3.5$ Å; this difference is

$$\delta\varepsilon_{\rm Coul}\equiv\varepsilon(2e)_{\rm Coul}-\varepsilon(b)_{\rm Coul}=\frac{U_0}{100}+1.11\ {\rm eV}\ , \tag{6.16}$$

which, for $U_0\sim 10$–20 eV, is larger than

$$\Delta\varepsilon+2K\cong 1.17\ {\rm eV}\ , \tag{6.17}$$

given by (6.6) and (6.7). Thus, as expected, the Coulomb energy within a Wigner-Seitz cell favors the boson band over the 3^- band.

C. van der Waals energy

The large polarizability of the C_{60} negative ion enhances the van der Waals energy.

Consider first $K_1^+C_{60}^-$, and assume that each Wigner-Seitz cell (say the ath cell) contains one valence electron at $\boldsymbol{\rho}_a$, whose distance from the lattice-site position $\mathbf{R}_a$ is $\mathbf{r}_a$; i.e.,

$$\boldsymbol{\rho}_a=\mathbf{R}_a+\mathbf{r}_a\ . \tag{6.18}$$

Expand the Coulomb energy

$$V_{\rm Coul}=\frac{e^2}{8\pi}\sum_{a,b}\frac{1}{\rho_{ab}}$$

into a power series in $\mathbf{r}_a$ (where $\rho_{ab}=|\boldsymbol{\rho}_a-\boldsymbol{\rho}_b|$ and the sum extends over all a and b independently, with $a\neq b$):

$$V_{\rm Coul}=V_{mm}+V_{md}+V_{mq}+V_{dd}+\cdots\ , \tag{6.19}$$

with the subscripts m, d, and q denoting monopole, dipole, and quadrupole. The monopole-monopole term V_{mm} is already included in the previous Madelung energy calculation; the monopole-dipole term V_{md} and the monopole-quadrupole term V_{mq} are zero in first-order perturbation because of the cubic symmetry of the lattice. The dipole-dipole interaction is

$$V_{dd}=\frac{e^2}{8\pi}\sum_{ab}R_{ab}^{-5}[R_{ab}^2\mathbf{r}_a\cdot\mathbf{r}_b-3(\mathbf{R}_{ab}\cdot\mathbf{r}_a)(\mathbf{R}_{ab}\cdot\mathbf{r}_b)]\ , \tag{6.20}$$

where $\mathbf{R}_{ab}=\mathbf{R}_a-\mathbf{R}_b$. The second-order perturbation of V_{dd} gives the van der Waals energy E_v. (The corresponding second-order effects of V_{md} and V_{mq} are unimportant because the off-diagonal matrix elements of the monopole connect $3^\pm$ only to excited states of the same quantum number; these have to lie beyond the molecular orbit spectrum of a single C_{60} molecule.)

Since we are interested in the energy of the 3^- band relative to the boson band, the van der Waals energy between the core electrons[17] of one C_{60} molecule and the core electrons of another C_{60} molecule is not relevant; that between one 3^- and the core electrons of a C_{60} molecule turns out to be rather small and can therefore be neglected. Because of the near degeneracy of the parity doublets, we consider only the transitions from two initial 3^- electrons (each on a different C_{60} molecule) to two 3^+ electrons and then back to the initial state, as shown in Fig. 2. All other diagrams are neglected. By using (3.20) and averaging all such initial states, we derive the van der Waals energy per C_{60} molecule in $K_1^+C_{60}^-$:

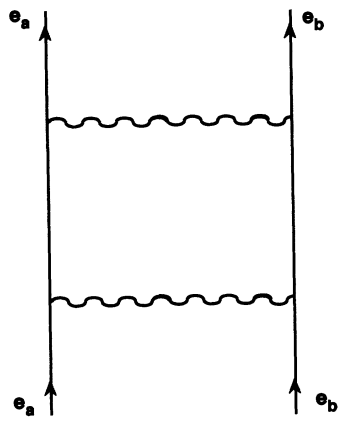

FIG. 2. Diagrams for the van der Waals energy between two electrons e_a and e_b, each on a different C_{60} molecule.

$$E_v(e)=-\frac{1}{2}\left[\frac{e^2}{4\pi}\right]^2\frac{R_0^4}{d^6}\frac{1}{\Delta\varepsilon}S\ , \tag{6.21}$$

where (e) on the left-hand side indicates that C_{60}^- has one extra e, $d\cong 2\sqrt{2}R$ is the distance between the nearest-neighboring C_{60} molecules, $\Delta\varepsilon=\varepsilon_+-\varepsilon_-$ is given by (6.6), and

$$S=\frac{2}{3}\sum{}'\frac{1}{(m^2+n^2+l^2)^3}=1.2045\ , \tag{6.22}$$

in which the sum $\sum'$ is over all integrals m, n, and l with $m+n+l=$even, excluding $m=n=l=0$.

Next, we consider $K_2^+C_{60}^{2-}$ and limit our analysis to two cases: (i) Every Wigner-Seitz cell contains two uncorrelated 3^- electrons, and (ii) every Wigner-Seitz cell contains one "boson" (i.e., two electrons in the $^1s_{-,\mathrm{sym}}$ state). We find the van der Waals energy per C_{60} molecule is, for case (i),

$$E_v(2e)=4E_v(e)\ . \tag{6.23}$$

For case (ii) the van der Waals energy is zero. This is because the operator $\mathbf{r}_a$ in the dipole-dipole interaction (6.20) has to bring the $^1s_{-,\mathrm{sym}}$ wave function (6.4) of the boson (in the ath Wigner-Seitz cell) into either $\hat{\mathbf{e}}_-(g)\times\hat{\mathbf{e}}_-(g')$ or $\hat{\mathbf{e}}_+(g)\times\hat{\mathbf{e}}_+(g')$; on account of Fermi statistics, both would require a total spin $\sigma=1$, which is uncoupled.

For $K_3^+C_{60}^{3-}$ we also consider only two cases: (i) Every Wigner-Seitz cell contains three uncorrelated 3^- electrons and (ii) every cell contains one boson and one uncorrelated 3^- electron. In case (i) the van der Waals energy per C_{60} molecule is

$$E_v(3e)=9E_v(e) \tag{6.24}$$

and, in case (ii),

$$E_v(be)=E_v(e)\ . \tag{6.25}$$

Setting $\Delta\varepsilon\cong 0.37$ eV, $d\cong 2\sqrt{2}R\cong 10$ Å, we obtain, from (6.21), (6.22), (6.24), and (6.25),

$$E_v(3e)\cong -0.40\ \text{eV} \tag{6.26a}$$

and

$$E_v(be)\cong -0.045\ \text{eV}\ . \tag{6.26b}$$

Combining these values with (6.16) and (6.17), we find that for K_3C_{60} the overall energy balance is

$$\delta\varepsilon_{\mathrm{Coul}}+E_v(3e)-E_v(be)-\Delta\varepsilon-2K=\frac{U_0}{100}-0.42\ \text{eV}\ , \tag{6.27}$$

which is -0.22 eV if U_0 is taken to be $\cong 20$ eV, slightly in favor of the 3^- band. Considering the very approximate nature of our estimates and that the balance (6.27) is only about 2% of the initial energy (6.9),

$$\varepsilon(3e)_{\mathrm{Coul}}\cong\tfrac{3}{100}U_0+10.7\ \text{eV}\ ,$$

which we start with, this final value cannot be relied upon. However, it does suggest the closeness of these two bands. As we shall see, the possibility that the boson band may well lie within the 3^- band and (quite likely) near its bottom portion can lead to several interesting consequences.

D. Screening

The reduction of Coulomb energy due to polarization charges is a form of electric screening. Phenomenologically, at short distances r, the overall effect is similar to the replacement of the Coulomb potential by an *ad hoc* Debye- (or Yukawa-) type potential

$$\frac{e^2}{4\pi r}e^{-\mu r/R_0}\ , \tag{6.28}$$

with μ as the screening parameter. [At long distances, (6.28) applies only when there are charge fluctuations.] Equation (6.16) then becomes

$$\delta\varepsilon_{\mathrm{Coul}}=\frac{U_0}{100}+\begin{cases}1.11\ \text{eV} & \text{for } \mu=0,\\ 0.80\ \text{eV} & \text{for } \mu=1,\\ 0.46\ \text{eV} & \text{for } \mu=2,\\ 0 & \text{for } \mu=\infty\ .\end{cases} \tag{6.29}$$

Since the Coulomb energy favors bosons, the effect of screening has to be the opposite. The reduction (6.26) due to the van der Waals energy is equivalent to having $\mu\cong 1$, i.e., a screening length $\cong 3.5$ Å.

VII. CHARGE FLUCTUATIONS

The Bloch wave number vector $\mathbf{k}$ carried by the fermionic and bosonic wave functions of (6.1) and (6.3) necessarily generates charge fluctuations in coordinate space. As we shall see, to a good approximation, the Coulomb energy within the same Wigner-Seitz cell produced by these charge fluctuations is compensated by the (negative) induced polarization energy between neighboring C_{60} ions, on account of their large polarizability. This enables us in Sec. VIII to examine the interplay between the fermion and boson bands and in Sec. IX to apply the concept of Bose-Einstein condensation to the

fermion-boson system. Throughout this section, $\mathbf{R}$ denotes the lattice-site position [i.e., $\mathbf{R}=\mathbf{R}_a$ in (6.1)–(6.3)].

We first review the types of charge fluctuations in our problem.

A. Ideal Bose condensate on a lattice

Let $b_{\mathbf{R}}$ be the bosonic annihilation operator defined on the lattice site $\mathbf{R}$; its Hermitian conjugate $b_{\mathbf{R}}^{\dagger}$ is the corresponding creation operator, with the commutator

$$[b_{\mathbf{R}'},b_{\mathbf{R}}^{\dagger}]=\delta_{\mathbf{R}\mathbf{R}'} . \tag{7.1}$$

Define

$$b_{\mathbf{k}}\equiv\frac{1}{\sqrt{\mathcal{N}}}\sum_{\mathbf{R}} e^{-i\mathbf{k}\cdot\mathbf{R}}b_{\mathbf{R}} , \tag{7.2}$$

where $\mathcal{N}$ is the total number of lattice sites and $\mathbf{k}$ is within the Brillouin zone; therefore,

$$b_{\mathbf{R}}=\frac{1}{\sqrt{\mathcal{N}}}\sum_{\mathbf{k}} e^{i\mathbf{k}\cdot\mathbf{R}}b_{\mathbf{k}} , \tag{7.3}$$

with the sum $\sum_{\mathbf{k}}$ extending over all $\mathbf{k}$ within the Brillouin zone.

Consider a system of N free bosons; its condensate is

$$|\ \rangle=\frac{1}{\sqrt{N!}}(b_0^{\dagger})^N|0\rangle , \tag{7.4}$$

where $|0\rangle$ is the vacuum state and $b_0=b_{\mathbf{k}}$ when $\mathbf{k}=0$. From (7.3) and (7.4), we see that the probability of finding n bosons on any site $\mathbf{R}$ is

$$P(n)=\frac{N!}{n!(N-n)!}\left[\frac{1}{\mathcal{N}}\right]^n\left[1-\frac{1}{\mathcal{N}}\right]^{N-n} ; \tag{7.5}$$

furthermore, the particle distributions on different sites are *uncorrelated*. Taking the limit $\mathcal{N}\to\infty$, but keeping the average

$$\bar{n}\equiv\frac{N}{\mathcal{N}}$$

fixed, we have the Poisson distribution

$$P(n)\to\frac{\bar{n}^{\,n}}{n!}e^{-\bar{n}} . \tag{7.6}$$

Its standard deviation squared is

$$\Delta n^2\equiv\overline{n^2}-\bar{n}^{\,2}=\bar{n} . \tag{7.7}$$

B. Bosons with an infinite (same site) repulsion

Let $U(\mathbf{R}-\mathbf{R}')$ be the interaction energy between two bosons at lattice sites $\mathbf{R}$ and $\mathbf{R}'$. Assume

$$U(\mathbf{R}-\mathbf{R}')=\infty \quad \text{when } \mathbf{R}=\mathbf{R}' , \tag{7.8}$$

but otherwise *arbitrary*. Consequently, any state vector of the Hamiltonian must satisfy

$$b_{\mathbf{R}}^2|\ \rangle=0 . \tag{7.9}$$

Let

$$n_{\mathbf{R}}(b)\equiv b_{\mathbf{R}}^{\dagger}b_{\mathbf{R}} . \tag{7.10}$$

From (7.1) and (7.9), we have

$$n_{\mathbf{R}}(b)^2|\ \rangle=n_{\mathbf{R}}(b)|\ \rangle . \tag{7.11}$$

A good measure of the density fluctuation at $\mathbf{R}$ is

$$\Delta n^2\equiv\langle\,|n_{\mathbf{R}}(b)^2|\,\rangle-\langle\,|n_{\mathbf{R}}(b)|\,\rangle^2=\bar{n}(1-\bar{n}) , \tag{7.12}$$

where

$$\bar{n}\equiv\langle\,|n_{\mathbf{R}}(b)|\,\rangle=\frac{N}{\mathcal{N}} .$$

The maximum of Δn^2 is $\frac{1}{4}$.

If $U(\mathbf{R},\mathbf{R}')=0$ when $\mathbf{R}\neq\mathbf{R}'$, then the condensate is proportional to the coefficient of z^N in

$$\prod_{\mathbf{R}}(1+zb_{\mathbf{R}}^{\dagger})|0\rangle ; \tag{7.13}$$

its particle distributions at different sites are again uncorrelated.

C. Fermions on a lattice

Let $a_{\mathbf{R},s}$ be the sth species fermionic annihilation operator on the lattice site $\mathbf{R}$. It satisfies the standard anticommutation relation with its Hermitian conjugate $a_{\mathbf{R},s}^{\dagger}$:

$$\{a_{\mathbf{R}',s'},a_{\mathbf{R},s}^{\dagger}\}=\delta_{\mathbf{R}\mathbf{R}'}\delta_{ss'} . \tag{7.14}$$

The corresponding occupation number operator is

$$n_{\mathbf{R},s}(f)\equiv a_{\mathbf{R},s}^{\dagger}a_{\mathbf{R},s} . \tag{7.15}$$

Because $a_{\mathbf{R},s}^2=0$, we have, as in (7.12), for any state vector $|\ \rangle$,

$$\begin{aligned}\Delta n_s^2&\equiv\langle\,|n_{\mathbf{R},s}(f)^2|\,\rangle-\langle\,|n_{\mathbf{R},s}(f)|\,\rangle^2\\&=\bar{n}_s(1-\bar{n}_s) ,\end{aligned} \tag{7.16}$$

where

$$\bar{n}_s=\langle\,|n_{\mathbf{R},s}|\,\rangle .$$

Define, as in (7.2),

$$a_{\mathbf{k},s}\equiv\frac{1}{\sqrt{\mathcal{N}}}\sum_{\mathbf{R}} e^{-i\mathbf{k}\cdot\mathbf{R}}a_{\mathbf{R},s} . \tag{7.17}$$

For applications to K_mC_{60}, neglecting the energy dispersion in the 3^- band, we assign $s=1,2,\ldots,6$ to denote the sixfold degeneracy (including spin) of the 3^- band. Assume the state vector to be that of a free degenerate Fermi sea:

$$|\rangle=\prod_{\mathbf{k}}\prod_{s=1}^{6}a_{\mathbf{k},s}^{\dagger}|\,\rangle , \tag{7.18}$$

where $\prod_{\mathbf{k}}'$ extends over the occupied portion of the Brillouin zone. Let

$$n_{\mathbf{R}}\equiv\sum_{s=1}^{6}n_{\mathbf{R},s} . \tag{7.19}$$

We have, for K_mC_{60} with $m\leq 6$,

$$\bar{n} \equiv \langle |n_{\mathbf{R}}| \rangle = m \ , \tag{7.20}$$

$\bar{n}_s = \bar{n}/6$, and, in accordance with (7.16),

$$\Delta n^2 \equiv \langle |n_{\mathbf{R}}^2| \rangle - \langle |n_{\mathbf{R}}| \rangle^2 = \bar{n}\left[1 - \frac{\bar{n}}{6}\right] . \tag{7.21}$$

The electronic fluctuations at different C_{60} sites are correlated, with the correlation function (for a spherical Fermi sea with Fermi momentum k_F and at $\mathbf{R} \neq \mathbf{R}'$) given by

$$\Delta^2_{\mathbf{R},\mathbf{R}'} \equiv \langle |n_{\mathbf{R}} n_{\mathbf{R}'}| \rangle - \bar{n}^2 = -\frac{3\tau^2 k_F^4}{2\pi^4 r^2} j_1^2(k_F r) \ , \tag{7.22}$$

where τ is the volume of a unit cell, $r = |\mathbf{R} - \mathbf{R}'|$, and $j_1(z) = (\sin z - z\cos z)/z^2$ is the first-order spherical Bessel function. For K_3C_{60}, $k_F \cong \frac{1}{2}$ Å^{-1}, and when $\mathbf{R}$ and $\mathbf{R}'$ are nearest neighbors,

$$\frac{\Delta^2_{\mathbf{R},\mathbf{R}'}}{\Delta n^2} \cong -0.028 \ , \tag{7.23}$$

indicating only weak correlations.

D. Coulomb energy

To show why such charge fluctuations do not cause serious energy imbalances, we consider the case of K_3C_{60} without bosons. Let $n = \bar{n} + \Delta n$ be the charge within a Wigner-Seitz cell (excluding K^+), where $\bar{n} = 3$ and, according to (7.21), the average of Δn squared is $\frac{3}{2}$. The corresponding electrostatic energy within the cell is

$$\langle \tfrac{1}{2} n(n-1) \rangle \varepsilon_{\text{pair}} \ , \tag{7.24}$$

with $\varepsilon_{\text{pair}}$ given by (6.8) and $\langle\ \rangle$ denoting the average. This causes an increase of Coulomb energy due to charge fluctuation,

$$[\langle \tfrac{1}{2} n(n-1) \rangle - \tfrac{1}{2}\bar{n}(\bar{n}-1)]\varepsilon_{\text{pair}} = \tfrac{3}{4}\varepsilon_{\text{pair}} \cong \frac{3U_0}{400} + 2.68 \text{ eV} \ , \tag{7.25}$$

which, as we shall see, is compensated by (i) Debye screening at large distances and (ii) the monopole-dipole term V_{md} in (6.19) at shorter distances (i.e., between neighboring C_{60} molecules).

In a Fermi sea of electrons, the Coulomb potential due to any charge fluctuation is screened at large distances when $r \gg \lambda_D$, where λ_D is the Debye length given by

$$\lambda_D^{-2} = m_e k_F e^2/\pi^2 \ , \tag{7.26}$$

with $\hbar = 1$. For K_3C_{60} and assuming m_e = mass of a free electron, we find λ_D to be quite small, $\cong 0.9$ Å. But for the applicability of the screened Debye potential $r^{-1}e^{-r/\lambda_D}$, the distance r has to be $> 8\lambda_D$.

Without charge fluctuations, because of cubic symmetry the monopole-dipole interaction V_{md} between neighboring C_{60} molecules vanishes in first-order perturbation, and as mentioned before in Sec. VI C, its second-order effect is unimportant. However, the situation becomes very different when there are charge fluctuations. The electric field produced by $e\Delta n$ on one C_{60} molecule polarizes all of its 12 nearest neighbors at distance d through V_{md}, giving a negative polarization energy

$$\delta E = -6\alpha \left[\frac{e\Delta n}{4\pi d^2}\right]^2 , \tag{7.27}$$

where α is the polarizability of C_{60}^{3-}. As discussed before, from (3.23)–(3.25), with $\Delta\varepsilon = \varepsilon_+ - \varepsilon_- \sim 0.37$ eV, the polarizability of a (singly ionized) C_{60}^- is already near the Clausius-Mossotti limit $\alpha_0 = 48R_0^3$, where, as before, $R_0 \cong 3.5$ Å is the C_{60} molecule radius. (If the $3e$ in C_{60}^{3-} could be polarized independently, its polarizability would greatly exceed the limit α_0.) Thus, as an estimate, we simply take $\alpha = \alpha_0$ for C_{60}^{3-}. This gives $\delta E \cong -2.21$ eV, with a magnitude comparable to (7.25). Without screening, the effect of including all distant C_{60} molecules is to multiply (7.27) by

$$S = \tfrac{1}{3}\sum (m_1^2 + m_2^2 + m_3^2)^{-2} \cong 2.1115 \ , \tag{7.28}$$

where the sum is over all integral m_i with $m_1 + m_2 + m_3 =$ even, excluding $m_1 = m_2 = m_3 = 0$; in that case, the total polarization energy $S\,\delta E$ would overcompensate (7.25). Of course, with the Debye screening this does not happen, but (7.25) can be reduced to nearly zero.

VIII. BOSON BAND

In this section we return to the two-particle correlated wave function (6.3) and examine, via the following simplified (but explicit) model, whether such a pair state can be generalized into a boson band in K_nC_{60}.

A. Model Hamiltonian

As in (7.17), let $a_{\mathbf{k},s}$ and $a^\dagger_{\mathbf{k},s}$ be the annihilation and creation operators of the electrons in the 3^- band, with the index

$$s = i,\sigma \tag{8.1}$$

denoting both the spin $\sigma = \uparrow$ or $\downarrow$ and the vector component $i = 1,2,3$. Likewise, $a'_{\mathbf{k},s}$ and $a'^\dagger_{\mathbf{k},s}$ are the corresponding operators of the 3^+ band. In coordinate space, on the lattice site $\mathbf{R}$, we have

$$a_{\mathbf{R},s} = \frac{1}{\sqrt{\mathcal{N}}} \sum_{\mathbf{k}} e^{i\mathbf{k}\cdot\mathbf{R}} a_{\mathbf{k},s} \tag{8.2a}$$

and

$$a'_{\mathbf{R},s} = \frac{1}{\sqrt{\mathcal{N}}} \sum_{\mathbf{k}} e^{i\mathbf{k}\cdot\mathbf{R}} a'_{\mathbf{k},s} \ , \tag{8.2b}$$

where, as well as in the following, the $\mathbf{k}$ sum extends only over the Brillouin zone. In this model the energy of these two bands is described by the Hamiltonian

$$H_0 = \sum_{\mathbf{k},s} [\varepsilon_k a^\dagger_{\mathbf{k},s} a_{\mathbf{k},s} + (\varepsilon_{\mathbf{k}} + \delta\varepsilon) a'^\dagger_{\mathbf{k},s} a'_{\mathbf{k},s}] \ , \tag{8.3}$$

with ε_k given by a band calculation. We assume the same ε_k for both bands, showing the parity-doublet structure;

within each band, there is a sixfold degeneracy indicated by the subscript s. The separation $\delta\varepsilon$ denotes the energy difference between, e.g., the bottoms of these two bands; thus, $\delta\varepsilon \approx \Delta\varepsilon + K \cong 0.77$ eV, given by (6.6) and (6.7).

The pairing states ${}^1s_{-,\mathrm{sym}}$ and ${}^1s_{+,\mathrm{asym}}$ of (4.27) at $\mathbf{R}$ are represented by

$$\phi_{\mathbf{R}}^{\dagger}|0\rangle \quad \text{and} \quad \phi_{\mathbf{R}}^{\prime\dagger}|0\rangle \ , \tag{8.4}$$

where $|0\rangle$ is the vacuum state,

$$\phi_{\mathbf{R}}^{\dagger} \equiv \sum_{i=1}^{3} \frac{1}{\sqrt{6}} (a_{\mathbf{R},i\uparrow}^{\dagger} a_{\mathbf{R},i\downarrow}^{\prime\dagger} + a_{\mathbf{R},i\uparrow}^{\prime\dagger} a_{\mathbf{R},i\downarrow}^{\dagger}) \tag{8.5}$$

may be regarded as the creation operator for a (bare) *pseudoscalar* field defined on the lattice, and

$$\phi_{\mathbf{R}}^{\prime\dagger} \equiv \sum_{i=1}^{3} \frac{1}{\sqrt{6}} (a_{\mathbf{R},i\uparrow}^{\dagger} a_{\mathbf{R},i\downarrow}^{\dagger} - a_{\mathbf{R},i\uparrow}^{\prime\dagger} a_{\mathbf{R},i\downarrow}^{\prime\dagger}) \tag{8.6}$$

the corresponding operator for a (bare) *scalar* field. Between states consisting of only 3^- electrons, the matrix elements of the commutator $[\phi_{\mathbf{R}}^{\dagger}, a_{\mathbf{k},s}]$ are all zero; the same does not hold for $[\phi_{\mathbf{R}}^{\prime\dagger}, a_{\mathbf{k},s}]$.

To simulate the low-energy preference of these pairing states at $\mathbf{R}$, we introduce

$$H_1 = -G \sum_{\mathbf{R}} \phi_{\mathbf{R}}^{\dagger} \phi_{\mathbf{R}} - G' \sum_{\mathbf{R}} \phi_{\mathbf{R}}^{\prime\dagger} \phi_{\mathbf{R}}^{\prime} \tag{8.7}$$

with G and G' both positive and approximately equal, in accordance with the parity-doublet nature. The total model Hamiltonian is

$$H = H_0 + H_1 \ . \tag{8.8}$$

B. Pseudoscalar band

We first discuss the modification to the pairing wave function (6.3) due to the 3^- and 3^+ band structure. Define a "pseudoscalar" state of total momentum

$$\mathbf{K} = \mathbf{k}_1 + \mathbf{k}_2 \tag{8.9}$$

by

$$|\mathrm{ps}\rangle = \sum_{\mathbf{k},i} f_{\mathbf{K}}(\mathbf{k}) (a_{\mathbf{k}_1,i\uparrow}^{\dagger} a_{\mathbf{k}_2,i\downarrow}^{\prime\dagger} + a_{\mathbf{k}_1,i\uparrow}^{\prime\dagger} a_{\mathbf{k}_2,i\downarrow}^{\dagger}) |0\rangle \tag{8.10}$$

and

$$\mathbf{k} = \tfrac{1}{2}(\mathbf{k}_1 - \mathbf{k}_2) \ , \tag{8.11}$$

with both $\mathbf{k}_1, \mathbf{k}_2$ within the Brillouin zone. The Schrödinger equation $H|\mathrm{ps}\rangle = E|\mathrm{ps}\rangle$ gives

$$f_{\mathbf{K}}(\mathbf{k}) = \frac{G}{\varepsilon_{\mathbf{k}_1} + \varepsilon_{\mathbf{k}_2} + \delta\varepsilon - E} \frac{A}{\mathcal{N}} \ , \tag{8.12}$$

where

$$A = \sum_{\mathbf{k}} f_{\mathbf{K}}(\mathbf{k}) \ . \tag{8.13}$$

Hence the eigenvalue E is determined by the roots of the secular equation

$$F(E) \equiv -1 + \frac{G}{\mathcal{N}} \sum_{\mathbf{k}} \frac{1}{\varepsilon_{\mathbf{k}_1} + \varepsilon_{\mathbf{k}_2} + \delta\varepsilon - E} = 0 \ . \tag{8.14}$$

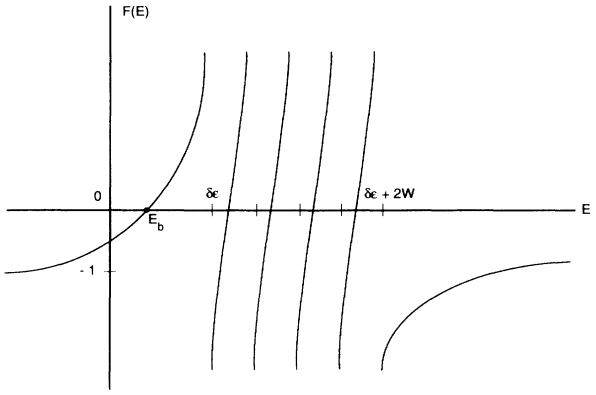

FIG. 3. Function $F(E)$ is defined by (8.14); it approaches -1 as $E \to \pm\infty$ and $F(E) \to \pm\infty$ as $E \to \varepsilon_{\mathbf{k}_1} + \varepsilon_{\mathbf{k}_2} + \delta\varepsilon \mp (0+)$. The roots $F(E)=0$ give the eigenvalues of $H|\mathrm{ps}\rangle = E|\mathrm{ps}\rangle$, with H and $|\mathrm{ps}\rangle$ given by (8.8) and (8.10).

For $\mathbf{K}=0$, $\varepsilon_{\mathbf{k}_1} = \varepsilon_{\mathbf{k}} = \varepsilon_{-\mathbf{k}} = \varepsilon_{\mathbf{k}_2}$. The denominator in the summand in (8.14) becomes $2\varepsilon_{\mathbf{k}} + \delta\varepsilon - E$. For a finite lattice, $2\varepsilon_{\mathbf{k}} + \delta\varepsilon$ has only discrete values, ranging from $\delta\varepsilon$ to $2W + \delta\varepsilon$, with W = the width of the $3^{\pm}$ band. As shown in Fig. 3, the lowest eigenvalue E is

$$E_b < \delta\varepsilon \ ; \tag{8.15}$$

higher up in energy, between every pair of successive $2\varepsilon_k + \delta\varepsilon$, there is one root E. All roots are less than $2W + \delta\varepsilon$, since, for $E > 2W + \delta\varepsilon$, $F(E)$ is < -1. There is a one-to-one correspondence between the $\mathcal{N}$ discrete values of $2\varepsilon_{\mathbf{k}} + \delta\varepsilon$ and the $\mathcal{N}$ roots of (8.14).

In the limit $\mathcal{N} \to \infty$, $F(E)$ becomes

$$F_{\infty}(E) = -1 + \frac{G}{(2\pi)^3} \int_B \frac{d^3k}{\varepsilon_{\mathbf{K}/2+\mathbf{k}} + \varepsilon_{\mathbf{K}/2-\mathbf{k}} + \delta\varepsilon - E} \ , \tag{8.16}$$

where the subscript B restricts the integral to within the Brillouin zone. In order to retain (8.15) in the limit we require, at $E = \delta\varepsilon$ and $\mathbf{K}=0$,

$$F_{\infty}(\delta\varepsilon) = -1 + \frac{G}{(2\pi)^3} \int_B \frac{d^3k}{2\varepsilon_{\mathbf{k}}} > 0 \ . \tag{8.17}$$

This ensures a stable pseudoscalar bound state $|b>$ of energy $E_b < \delta\varepsilon$ in the model; its $\mathbf{K}$ dependence (and therefore also the boson band structure) can be determined by $F_{\infty}(E)=0$ for $\mathbf{K} \neq 0$. At any given $\mathbf{K}$, there is a cut on the real E axis, which, for $\mathbf{K}=0$, extends between $\delta\varepsilon$ and $2W + \delta\varepsilon$. In the complex E plane, for E infinitesimally

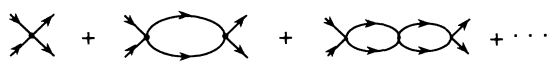

FIG. 4. Sum of Feynman diagrams for the two-particle state, bound or scattering.

above the cut, the state vector (8.10) is one with an outgoing scattering wave. In terms of the standard Feynman diagrams, the above exact solution is equivalent to the sum over an infinite series of bubble diagrams shown in Fig. 4.

It is of interest to examine the coordinate representation of the pseudoscalar state by expressing (8.10) in the form

$$|\mathrm{ps}\rangle=\sum_{\mathbf{R}}\frac{1}{\sqrt{\mathcal{N}}}e^{-i\mathbf{K}\cdot\mathbf{R}}\Phi_{\mathbf{R}}^{\dagger}|0\rangle\ , \tag{8.18}$$

where

$$\Phi_R^{\dagger}=\sum_{\mathbf{r}}\sum_{\mathbf{k}}\frac{1}{\mathcal{N}}f_{\mathbf{K}}(\mathbf{k})e^{-i\mathbf{k}\cdot\mathbf{r}}(a_{\mathbf{R}+(1/2)\mathbf{r},i\uparrow}^{\dagger}a_{\mathbf{R}-(1/2)\mathbf{r},i\downarrow}^{\prime\dagger}+a_{\mathbf{R}+(1/2)\mathbf{r},i\uparrow}^{\prime\dagger}a_{\mathbf{R}-(1/2)\mathbf{r},i\downarrow}^{\dagger})\ . \tag{8.19}$$

One may regard $\phi_{\mathbf{R}}^{\dagger}$ of (8.5) as the "bare" boson creation operator and $\Phi_R^{\dagger}$ as the "dressed" one. The scale of the $\mathbf{r}$ extension, after the first summation $\Sigma_{\mathbf{k}}$ in (8.19), for $\varepsilon_{\mathbf{k}}=k^2/2m$ is

$$a\cong[2m(\delta\varepsilon-E_b)]^{-1/2}\ . \tag{8.20}$$

Thus the operator $\Phi_R^{\dagger}$ and its Hermitian conjugate $\Phi_{\mathbf{R}}$ are well localized in the coordinate space. These operators can be used to construct a boson band for the crystal [as exemplified by the operators $b_R^{\dagger},b_R$ and $b_{\mathbf{k}}^{\dagger},b_{\mathbf{k}}$ in (7.1)–(7.13)].

When there is a partially filled 3^- band of top Fermi energy ε_F, an approximate solution of the pseudoscalar boson band can be obtained by summing over the same infinite series of bubble diagrams in Fig. 4, but replacing the Feynman propagator in vacuum by that in a Fermi sea. The result is simply to impose on the integral $\int_B d^3k$ in (8.16) and (8.17) a further constraint:

$$\varepsilon_{\mathbf{k}}>\varepsilon_F\ . \tag{8.21}$$

In Sec. VI we estimated that the energy balance (6.27) may be slightly negative, in favor of two electrons in the 3^- band (over the pseudoscalar boson). This implies, in this model,

$$E_b>0\ . \tag{8.22}$$

Thus, in addition to the lower bound of G determined by (8.17), there is also an upper bound given by

$$F_{\infty}(0)=-1+\frac{G}{(2\pi)^3}\int_B\frac{d^3k}{2\varepsilon_k+\delta\varepsilon}<0\ . \tag{8.23}$$

In the model we have the selection rule for the pseudoscalar boson b:

$$b\not\to 3^-+3^-\ , \tag{8.24}$$

where each 3^- stands for an electron in the 3^- band. In the realistic case, a *weak* transition exists between 3^-+3^+ and 3^-+3^-. Hence there is a violation of (8.24). The bosons are metastable if the top energy ε_F of the Fermi sea is $<\frac{1}{2}E_b$, but stable otherwise. Furthermore, ε_F does not rise above $\frac{1}{2}E_b$, until the boson band is filled.

C. Scalar band

Similar to (8.10), we can construct a scalar state of total momentum $\mathbf{K}=\mathbf{k}_1+\mathbf{k}_2$:

$$|\mathrm{sc}\rangle=\sum_{\mathbf{k},i}[g_{\mathbf{K}}(\mathbf{k})a_{\mathbf{k}_1,i\uparrow}^{\dagger}a_{\mathbf{k}_2,i\downarrow}^{\dagger}-h_{\mathbf{K}}(\mathbf{k})a_{\mathbf{k}_1,i\uparrow}^{\prime\dagger}a_{\mathbf{k}_2,i\downarrow}^{\prime\dagger}]|0\rangle\ , \tag{8.25}$$

where, as in (8.11), $\mathbf{k}=\frac{1}{2}(\mathbf{k}_1-\mathbf{k}_2)$. The Schrödinger equation

$$H|\mathrm{sc}\rangle=E'|\mathrm{sc}\rangle \tag{8.26}$$

gives

$$g_{\mathbf{K}}(\mathbf{k})=\frac{G'}{\varepsilon_{\mathbf{k}_1}+\varepsilon_{\mathbf{k}_2}-E'}\frac{A'}{\mathcal{N}} \tag{8.27}$$

and

$$h_{\mathbf{K}}(\mathbf{k})=\frac{G'}{\varepsilon_{\mathbf{k}_1}+\varepsilon_{\mathbf{k}_2}+2\delta\varepsilon-E'}\frac{A'}{\mathcal{N}}\ , \tag{8.28}$$

with

$$A'=\tfrac{1}{2}\sum_{\mathbf{k}}[g_{\mathbf{K}}(\mathbf{k})+h_{\mathbf{K}}(\mathbf{k})]\ . \tag{8.29}$$

Hence the eigenvalue E' is determined by the roots of

$$F'(E')\equiv-1+\frac{G'}{2\mathcal{N}}\sum_{\mathbf{k}}\left[\frac{1}{\varepsilon_{\mathbf{k}_1}+\varepsilon_{\mathbf{k}_2}-E'}+\frac{1}{\varepsilon_{\mathbf{k}_1}+\varepsilon_{\mathbf{k}_2}+2\delta\varepsilon-E'}\right]=0\ . \tag{8.30}$$

For $\mathbf{K}=0$, (8.30) becomes

$$F'(E')=-1+\frac{G'}{2\mathcal{N}}\sum_{\mathbf{k}}\left[\frac{1}{2\varepsilon_{\mathbf{k}}-E'}+\frac{1}{2(\varepsilon_{\mathbf{k}}+\delta\varepsilon)-E'}\right]=0\ . \tag{8.31}$$

Similar to (8.15), the lowest eigenvalue is

$$E_b'<0\ ; \tag{8.32}$$

between every successive pair of $2\varepsilon_k$ and $2(\varepsilon_k+\delta\varepsilon)$ in an ascending order of energy, one has an eigenvalue E'. Hence there is a one-to-one correspondence between the $2\mathcal{N}$ discrete values of $2\varepsilon_k$ and $2(\varepsilon_k+\delta\varepsilon)$ and the $2\mathcal{N}$ roots of $F'(E')=0$. In accordance with the fermionic band calculation[16] which shows no overlap between the 3^- and 3^+ bands, we assume

$$\delta\varepsilon>W\ , \tag{8.33}$$

where, as before, W is the $3^{\pm}$ band width. Consequently, there is always one (and only one) root $E'=E_b''$, with

$$2\delta\varepsilon > E_b'' > 2W \ . \tag{8.34}$$

In the limit $\mathcal{N}\to\infty$, $F'(E')$ becomes $F'_\infty(E')$. There are several possibilities, depending on the values of $F'_\infty(E')$ at $E'=0$ and $2\delta\varepsilon$:

$$F'_\infty(0)=-1+\frac{G'}{16\pi^3}\int_B d^3k\left[\frac{1}{2\varepsilon_k}+\frac{1}{2(\varepsilon_k+\delta\varepsilon)}\right] \tag{8.35}$$

and

$$F'_\infty(2\delta\varepsilon)=-1+\frac{G'}{16\pi^3}\int_B d^3k\left[\frac{1}{2(\varepsilon_{\mathbf{k}}-\delta\varepsilon)}+\frac{1}{2\varepsilon_{\mathbf{k}}}\right] , \tag{8.36}$$

for $\mathbf{K}=0$; on account of (8.33),

$$F'_\infty(0) > F'_\infty(2\delta\varepsilon) \ . \tag{8.37}$$

(i) $F'_\infty(0)>F'_\infty(2\delta\varepsilon)>0$. In this case both (8.32) and (8.34) survive in the limit $\mathcal{N}\to\infty$. There is a scalar bound state with $E_b'<0$; in addition, there is a second excited "stable" state of energy E_b'' between $2W$ and $2\delta\varepsilon$. The inequality $E_b''>2W$ prevents its decay into two 3^- electrons, and the other inequality $E_b''<2\delta\varepsilon$ makes its decay into two 3^+ electrons impossible.

(ii) $F'_\infty(0)>0$, *but* $F'_\infty(2\delta\varepsilon)<0$. There remains a bound state with $E_b'<0$ in this case, but there is no second stable state.

(iii) $F'_\infty(0)<0$. Therefore (8.32) becomes

$$E_b'\to 0 \tag{8.38}$$

in the limit of an infinite lattice; the bound state also disappears.

As in (8.19), we can construct a "dressed" scalar boson creation operator

$$\Phi'^{\dagger}_{\mathbf{R}}\equiv\sum_{\mathbf{r}}\sum_{\mathbf{k}}\frac{1}{\mathcal{N}}[g_{\mathbf{K}}(\mathbf{k})e^{-i\mathbf{k}\cdot\mathbf{r}}a^{\dagger}_{\mathbf{R}+(1/2)\mathbf{r},i\uparrow}a^{\dagger}_{\mathbf{R}-(1/2)\mathbf{r},i\downarrow}-h_{\mathbf{K}}(\mathbf{k})e^{-i\mathbf{k}\cdot\mathbf{r}}a'^{\dagger}_{\mathbf{R}+(1/2)\mathbf{r},i\uparrow}a'^{\dagger}_{\mathbf{R}-(1/2)\mathbf{r},i\downarrow}] \ . \tag{8.39}$$

In cases (i) and (ii), $E_b'<0$, and similar to (8.20), the scale of the $\mathbf{r}$ extension in $\Phi'^{\dagger}_{\mathbf{R}}$, after the first summation, is

$$a'\cong(-2mE_b')^{-1/2} \ . \tag{8.40}$$

The scalar boson band is a valid concept.

In case (iii), in accordance with (8.38), $E_b'=0$ as $\mathcal{N}\to\infty$. Hence $a'\to\infty$ and the operator $\Phi'_{\mathbf{R}}$ becomes unbounded (in the coordinate space). We cannot meaningfully apply the concept of a scalar boson band.

IX. SUPERCONDUCTIVITY

In the model given in the previous section, there can be two different long-range order parameters, as we shall see. From $\phi_{\mathbf{R}}$ and $\phi'_{\mathbf{R}}$, defined by the Hermitian conjugates of (8.5) and (8.6), we can construct the following momentum-space operators:

$$\phi_{\mathbf{k}}=\frac{1}{\sqrt{\mathcal{N}}}\sum_{\mathbf{R}}e^{-i\mathbf{k}\cdot\mathbf{R}}\phi_{\mathbf{R}} \tag{9.1a}$$

and

$$\phi'_{\mathbf{k}}=\frac{1}{\sqrt{\mathcal{N}}}\sum_{\mathbf{R}}e^{-i\mathbf{k}\cdot\mathbf{R}}\phi'_{\mathbf{R}} \ , \tag{9.1b}$$

where, as before, $\mathbf{R}$ goes over all the $\mathcal{N}$ lattice sites and $\mathbf{k}$ is restricted to the Brillouin zone. Any state vector having a nonzero expectation value for $\phi_{\mathbf{k}}$ or $\phi'_{\mathbf{k}}$ at $\mathbf{k}=0$ (in the limit $\mathcal{N}\to\infty$) belongs to the superphase. Let

$$B_{\mathrm{ps}}\equiv\lim_{\mathcal{N}\to\infty}\langle|\phi_{\mathbf{k}=0}|\rangle \tag{9.2}$$

and

$$B_{\mathrm{sc}}\equiv\lim_{\mathcal{N}\to\infty}\langle|\phi'_{\mathbf{k}=0}|\rangle \ . \tag{9.3}$$

In this section we discuss briefly the different roles of these two long-range order parameters.

A. Scalar dominance

For states with $B_{\mathrm{sc}}\neq 0$, but $B_{\mathrm{ps}}=0$, the quasiparticle spectrum for the 3^- band has the typical BCS form, as can be derived by following the standard method,

$$[\omega_{\mathbf{k}}^2+\tfrac{1}{6}|G'B_{\mathrm{sc}}|^2]^{1/2} \ , \tag{9.4}$$

where

$$\omega_{\mathbf{k}}=\varepsilon_{\mathbf{k}}-\mu \ , \tag{9.5}$$

with μ=Fermi energy. The corresponding spectrum for the 3^+ band is

$$[(\omega_{\mathbf{k}}+\delta\varepsilon)^2+\tfrac{1}{6}|G'B_{\mathrm{sc}}|^2]^{1/2} \ . \tag{9.6}$$

B. Pseudoscalar dominance

For states with $B_{\mathrm{ps}}\neq 0$, but $B_{\mathrm{sc}}=0$, the boson band can become a physical reality. The system exhibits several characteristic features of the boson-fermion model,[18] even though the transition between two 3^- electrons to the pseudoscalar state ${}^1\mathbf{s}_{-,\mathrm{sym}}$ is a weak one. The most interesting possibility is when the excitation energy 2ν of the pseudoscalar boson equals 2 times the Fermi energy of the 3^- band:

$$2\nu=2\mu \ . \tag{9.7}$$

In this case the bosons become stable; the long-range order $B_{\mathrm{ps}}\neq 0$ can then be regarded as the result of a Bose-Einstein condensation.

C. Variation of T_c vs lattice size

In the case of pseudoscalar dominance with Bose-Einstein condensation, we can relate the long-range order parameter B_{ps} to the number N_0 of bosons with zero momentum in the condensate:

$$\frac{N_0}{\mathcal{N}}=|B_{ps}|^2 . \tag{9.8}$$

From (6.24)–(6.27), the excitation energy of the boson in K_3C_{60} can be written as

$$2\nu=-\frac{U_0}{100}+0.065\ \text{eV}+4\left[\frac{e^2}{4\pi}\right]^2\frac{R_0^4}{d^6}\frac{1}{\Delta\varepsilon}S , \tag{9.9}$$

in which the last term $4(e^2/4\pi)^2(R_0^4/d^6\Delta\varepsilon)S$ is simply $-E_v(3e)+E_v(be)$ with R_0, d, $\Delta\varepsilon$, and S given by (6.21) and (6.22); hence, for $-E(3e)+E_v(be)=0.355$ eV, (9.9) becomes

$$2\nu=-\frac{U_0}{100}+0.42\ \text{eV} , \tag{9.10}$$

which is the negative of (6.27). As the distance d between neighboring C_{60} molecules increases, the electrostatic screening weakens, which enhances the Coulomb energy, in favor of the boson; accordingly, the boson excitation energy 2ν decreases. From (9.9) we have

$$\frac{\partial\ln\nu}{\partial\ln d}=-\frac{1}{2\nu}\left[2\nu+\frac{U_0}{100}-0.065\ \text{eV}\right]6 , \tag{9.11}$$

which, for $U_0\cong 20$ eV and $2\nu\cong 0.22$ eV, gives

$$\frac{\partial\ln\nu}{\partial\ln d}\cong -10 . \tag{9.12}$$

The total charge density n (in units of e per volume) is carried partly by the bosons of density n_b and partly by the fermions of density n_f (in the 3^- band), with

$$n=n_f+2n_b . \tag{9.13}$$

Assuming (9.7) and for an ideal boson-fermion system, we have

$$n_b\propto T_c^{3/2} \tag{9.14a}$$

and

$$n_f\propto\mu^{3/2}=\nu^{3/2} , \tag{9.14b}$$

where T_c is the critical temperature. By using $\partial\ln n/\partial\ln d=-3$ and (9.13) and (9.14), we find

$$\frac{\partial\ln T_c}{\partial\ln d}=\frac{2}{3}\frac{\partial\ln n_b}{\partial\ln d}=-\frac{1}{n_b}\left[n+\frac{1}{2}n_f\frac{\partial\ln\nu}{\partial\ln d}\right] . \tag{9.15}$$

The experimental result[6] yields

$$\frac{\partial\ln T_c}{\partial\ln d}\cong 26 , \tag{9.16}$$

which, when combined with (9.12) and (9.13), gives

$$\frac{2n_b}{n}\cong\frac{2}{9} ; \tag{9.17}$$

i.e., about $\frac{7}{9}$ of the charge is carried by the fermions and $\frac{2}{9}$ by the bosons.

It has been pointed out[6] that BCS theory is consistent with the experimental observation of T_c increasing with d; the above discussion shows that the same is true when bosons dominate.

The general case when both B_{ps} and B_{sc} are nonzero will be discussed in a separate paper.

ACKNOWLEDGMENTS

This research was supported in part by the U.S. Department of Energy under Grants Nos. DE-FG02-92 ER40699 and DE-AC02-87 ER40325, Task B.

APPENDIX: MADELUNG ENERGY OF K_3C_{60}

The crystal structure of K_3C_{60} can be understood in terms of two simple cubic lattices A and B. The sites of the lattice A (referred to as A sites) are given by

$$\mathbf{R}_A=(n_1\hat{\mathbf{x}}_1+n_2\hat{\mathbf{y}}+n_3\hat{\mathbf{z}})a , \tag{A1}$$

and those of the lattice B (referred to as B sites) are given by

$$\mathbf{R}_B=[(n_1'+\tfrac{1}{2})\hat{\mathbf{x}}+(n_2'+\tfrac{1}{2})\hat{\mathbf{y}}+(n_3'+\tfrac{1}{2})\hat{\mathbf{z}}]a , \tag{A2}$$

where $a\cong 7.1$ Å and $n_1,n_2,n_3,n_1',n_2',n_3'$ are integers. The C_{60}^{3-} ions occupy half of the A sites, say, with $n_1+n_2+n_3=$even; the octahedral K^+ ions occupy the other half of the A sites, and the other (called tetrahedral) K^+ ions occupy all the B sites.

The Madelung energy per unit cell is

$$E_M=\tfrac{1}{2}e(-3V_{C_{60}}+V_{K^+}+V'_{K^+}+V''_{K^+}) , \tag{A3}$$

where $V_{C_{60}}$ is the electrostatic potential at a C_{60}^{3-} ion, V_{K^+} is the electrostatic potential at an octahedral K^+, and V'_{K^+},V''_{K^+} are the electrostatic potentials at two tetrahedral sites in a unit cell. The potential produced by an ion on its own site is excluded in the definitions of V in (A3), since the Madelung energy includes only the mutual Coulomb interactions, and the factor $\frac{1}{2}$ in (A3) is introduced so that each pair of ions is counted once.

The potential at a C_{60}^{3-} ion reads

$$\begin{aligned}V_{C_{60}}=&-\frac{3e}{4\pi a}\sum_{n_1n_2n_3}{}'\frac{1+(-)^{n_1+n_2+n_3}}{2R_n}e^{-\mu R_n}\\&+\frac{e}{4\pi a}\sum_{n_1n_2n_3}{}'\frac{1-(-)^{n_1+n_2+n_3}}{2R_n}e^{-\mu R_n}\\&+\frac{e}{4\pi a}\sum_{n_1n_2n_3}\frac{e^{-\mu R_n'}}{R_n'} ,\end{aligned} \tag{A4}$$

where $R_n\equiv(n_1^2+n_2^2+n_3^2)^{1/2}$,

$$R_n'\equiv[(n_1+\tfrac{1}{2})^2+(n_2+\tfrac{1}{2})^2+(n_3+\tfrac{1}{2})^2]^{1/2} ,$$

and $\sum'_{n_1n_2n_3}$ excludes the term with $n_1=n_2=n_3=0$. The

first sum of (A4) accounts for the potential produced by all other C_{60} ions, the second sum for that produced by octahedral K^+ ions, and the third for that produced by tetrahedral K^+ ions. The regularization parameter μ renders each sum convergent separately and will be set to zero after combining all the sums. Similarly, we can write the potentials at K^+ sites

$$V_{K^+}=-\frac{3e}{4\pi a}\sum_{n_1n_2n_3}{}'\frac{1-(-)^{n_1+n_2+n_3}}{2R_n}e^{-\mu R_n}+\frac{e}{4\pi a}\sum_{n_1n_2n_3}{}'\frac{1+(-)^{n_1+n_2+n_3}}{2R_n}e^{-\mu R_n}+\frac{e}{4\pi a}\sum_{n_1n_2n_3}\frac{e^{-\mu R_n'}}{R_n'}, \tag{A5}$$

$$V'_{K^+}+V''_{K^+}=\frac{2e}{4\pi a}\sum_{n_1n_2n_3}{}'\frac{e^{-\mu R_n}}{R_n}-\frac{3e}{4\pi a}\sum_{n_1n_2n_3}\frac{e^{-\mu R_n'}}{R_n'}+\frac{e}{4\pi a}\sum_{n_1n_2n_3}\frac{e^{-\mu R_n'}}{R_n'}. \tag{A6}$$

Substituting (A4)–(A6) into (A3), we obtain

$$E_M=\frac{e^2}{2\pi a}\left[\sum_{n_1n_2n_3}{}'\frac{e^{-\mu R_n}}{R_n}-\sum_{n_1n_2n_3}\frac{e^{-\mu R_n'}}{R_n'}\right]+\frac{e^2}{\pi a}\sum_{n_1n_2n_3}(-)^{n_1+n_2+n_3}\frac{e^{-\mu R_n}}{R_n}. \tag{A7}$$

The series in (A7) can be evaluated by means of the technique in Ref. 15. On account of the cubic symmetry, we have

$$\sum_{n_1n_2n_3}{}'\frac{1}{R_n}f(n_1n_2n_3)=3\sum_{n_1n_2n_3}{}'\frac{n_3^2}{R_n^3}f(n_1n_2n_3), \tag{A8}$$

$$\sum_{n_1n_2n_3}\frac{1}{R_n'}f(n_1n_2n_3)=3\sum_{n_1n_2n_3}\frac{(n_3+\frac{1}{2})^2}{R_n'^3}f(n_1n_2n_3), \tag{A9}$$

with any symmetric function $f(n_1n_2n_3)$ of $n_1n_2n_3$; hence, (A7) can be written as

$$E_M=\frac{3e^2}{\pi a}\left[\sum_{n_3=1}^{\infty}n_3^2\mathcal{G}(n_3)-\sum_{n_3=0}^{\infty}(n_3+\tfrac{1}{2})^2\mathcal{G}'(n_3)+2\sum_{n_3=1}^{\infty}(-)^{n_3}\mathcal{H}(n_3)\right], \tag{A10}$$

where

$$\mathcal{G}(n_3)=\int d^2\rho\frac{e^{-\mu(\rho^2+n_3^2)^{1/2}}}{(\rho^2+n_3^2)^{3/2}}\sum_{\mathbf{n}}\delta^2(\boldsymbol{\rho}-\mathbf{n}), \tag{A11}$$

$$\mathcal{G}'(n_3)=\int d^2\rho\frac{e^{-\mu[\rho^2+(n_3+1/2)^2]^{1/2}}}{[\rho^2+(n_3+\frac{1}{2})^2]^{3/2}}\sum_{\mathbf{n}}\delta^2(\boldsymbol{\rho}-\mathbf{n}'), \tag{A12}$$

and

$$\mathcal{H}(n_3)=\int d^2\rho\frac{e^{-\mu(\rho^2+n_3^2)^{1/2}}}{(\rho^2+n_3^2)^{3/2}}\sum_{\mathbf{n}}(-)^{n_1+n_2}\delta^2(\boldsymbol{\rho}-\mathbf{n}), \tag{A13}$$

with $\mathbf{n}\equiv(n_1,n_2)$, $\mathbf{n}'\equiv(n_1+\frac{1}{2},n_2+\frac{1}{2})$, and the sum $\sum_{\mathbf{n}}$ extending over all integrals n_1 and n_2. Using Poisson formulas

$$\sum_{\mathbf{n}}\delta^2(\boldsymbol{\rho}-\mathbf{n})=\sum_{\mathbf{m}}e^{i2\pi\mathbf{m}\cdot\mathbf{n}}, \tag{A14}$$

$$\sum_{\mathbf{n}}(-)^{n_1+n_2}\delta^2(\boldsymbol{\rho}-\mathbf{n})=\sum_{\mathbf{m}}e^{i2\pi\mathbf{m}'\cdot\mathbf{n}}, \tag{A15}$$

and

$$\sum_{\mathbf{n}}\delta^2(\boldsymbol{\rho}-\mathbf{n}')=\sum_{\mathbf{m}}(-)^{m_1+m_2}e^{i2\pi\mathbf{m}\cdot\mathbf{n}'}, \tag{A16}$$

with $\mathbf{m}\equiv(m_1,m_2)$, $\mathbf{m}'\equiv(m_1+\frac{1}{2},m_2+\frac{1}{2})$, and the sum $\sum_{\mathbf{m}}$ extending over all integrals m_1 and m_2. Equations (A11)–(A13) become

$$\mathcal{G}(n_3)=g_0(n_3)+\sum_{\mathbf{m}}g_{\mathbf{m}}(n_3), \tag{A17}$$

$$\mathcal{G}'(n_3)=g_0(n_3+\tfrac{1}{2})+\sum_{\mathbf{m}}{}'(-)^{m_1+m_2}g_{\mathbf{m}}(n_3+\tfrac{1}{2}), \tag{A18}$$

and

$$\mathcal{H}(n_3)=\sum_{\mathbf{m}}g_{\mathbf{m}'}(n_3), \tag{A19}$$

where

$$g_\kappa(z)=\int d^2\rho\frac{e^{-\mu(\rho^2+z^2)^{1/2}+i\boldsymbol{\kappa}\cdot\boldsymbol{\rho}}}{(\rho^2+z^2)^{3/2}}, \tag{A20}$$

$g_0(z)$ is $g_\kappa(z)$ and $\kappa=0$ and $\sum'_{\mathbf{m}}$ excludes the term with $m_1=m_2=0$. Except for the first term of (A17) and the first term of (A18), μ can be set to zero before summing over n_3, and $g_\kappa(z)$ is then an elementary function:

$$g_\kappa(z)=\frac{2\pi}{|z|}e^{-\kappa|z|}. \tag{A21}$$

Substituting (A17)–(A19) and (A21) into (A10), we end up with

$$E_M=\frac{e^2}{4\pi a}\left[C+6\pi\sum_{\mathbf{m}}{}'\frac{1-(-)^{m_1+m_2}\cosh\pi m}{\sinh^2\pi m}-12\pi\sum_{\mathbf{m}}\frac{1}{\cosh^2\pi m'}\right], \tag{A22}$$

where $m=(m_1^2+m_2^2)^{1/2}$,

$$m'=[(m_1+\tfrac{1}{2})^2+(m_2+\tfrac{1}{2})^2]^{1/2}\ ,$$

and

$$\begin{aligned}C&=12\lim_{\mu\to 0}\left[\sum_{n_3=1}^{\infty}n_3^2 g_0(n_3)-\sum_{n_3=0}^{\infty}(n_3+\tfrac{1}{2})^2 g_0(n_3+\tfrac{1}{2})\right]\\&=24\pi\lim_{\mu\to 0}\left[\sum_{n_3=1}^{\infty}n_3\int_1^{\infty}dx\frac{e^{-\mu n_3 x}}{x^2}-\sum_{n_3=0}^{\infty}(n_3+\tfrac{1}{2})\int_1^{\infty}dx\frac{e^{-\mu(n_3+\frac{1}{2})x}}{x^2}\right]\\&=6\pi\lim_{\mu\to 0}\int_1^{\infty}\frac{dx}{x^2}\,\frac{1-\cosh\frac{1}{2}\mu x}{\sinh^2\frac{1}{2}\mu x}=-3\pi\ .\end{aligned}\tag{A23}$$

Equations (5.2) and (5.3) for the Madelung energy of K_3C_{60} are thus established.

To estimate the upper bound of the Madelung energy of K_1C_{60} and K_2C_{60}, we simply remove all the tetrahedral K^+ ions in the case of K_1C_{60} and all the octahedral K^+ ions in the case of K_2C_{60}. The rest of the estimation follows the same steps from (A7)–(A23).

[1] H. W. Kroto *et al.*, Nature **318**, 162 (1985); W. Krätschmer *et al.*, *ibid.* **347**, 354 (1990); H. Ajie *et al.*, J. Phys. Chem. **94**, 8630 (1990).

[2] A. F. Hebard *et al.*, Nature **350**, 600 (1991).

[3] M. J. Rosseinsky *et al.*, Phys. Rev. Lett. **66**, 2830 (1991).

[4] K. Holczer *et al.*, Science **252**, 1154 (1991).

[5] K. Holczer *et al.*, Phys. Rev. Lett. **67**, 271 (1991).

[6] G. Sparn *et al.*, Science **252**, 1829 (1991); R. M. Fleming *et al.*, Nature **352**, 787 (1991); O. Zhou *et al.*, Science **255**, 833 (1992).

[7] P.-M. Allemand *et al.*, Science **253**, 301 (1991).

[8] S. Chakravarty, M. P. Gelfand, and S. Kivelson, Science **254**, 970 (1991) and unpublished.

[9] M. Hamermesh, *Group Theory and Its Application to Physical Problems* (Addison-Wesley, Reading, MA, 1962).

[10] F. Albert Cotton, *Chemical Applications of Group Theory*, 2nd ed. (Wiley-Interscience, New York, 1963).

[11] F. Hund, Z. Phys. **73**, 1 565 (1932); R. S. Mulliken, J. Chem. Phys. **1**, 492 (1933); E. Hückel, *ibid.* **72**, 310 (1931); **76**, 628 (1932); **83**, 632 (1933).

[12] D. A. Bochvar and E. G. Gal'pern, Dokl. Akad. Nauk SSSR **209**, 239 (1973).

[13] R. C. Haddon, L. E. Brus, and K. Raghavachari, Chem. Phys. Lett. **125**, 459 (1986).

[14] P. W. Stephens *et al.*, Nature **351**, 632 (1991).

[15] R. Friedberg and T. D. Lee, Phys. Rev. B **39**, 482 (1989).

[16] Y. N. Xu, M. Z. Huang, and W. Y. Ching, J. Chem. Phys. **96**, 1648 (1992); Phys. Rev. B **44**, 13 171 (1991); S. Saito and A. Oshiyama, *ibid.* **44**, 11 536 (1991).

[17] S. Saito and A. Oshiyama, Phys. Rev. Lett. **66**, 2637 (1991).

[18] R. Friedberg and T. D. Lee, Phys. Rev. B **40**, 6745 (1989); R. Friedberg, T. D. Lee, and H. C. Ren, *ibid.* **42**, 4122 (1990).